

PHOTOCATALYTIC AND ANTIBACTERIAL ACTIVITY OF SILVER NANOPARTICLES SYNTHESIZED USING GREEN APPROACH

A DISSERTATION

SUBMITTED IN PARTIAL FULFILLMENT OF THE REQUIREMENTS
FOR THE AWARD OF THE DEGREE

OF

MASTER'S IN PHYSICS

[PHYSICS]

Submitted by:

RUBY (2K19/MSCPHY/22)
ARYAN (2K19/MSCPHY/32)

Under the supervision of

Dr. Mohan Singh Mehata



Department of Applied Physics

DELHI TECHNOLOGICAL UNIVERSITY

(Formerly Delhi College of Engineering)

Bawana Road, Delhi-110042

MAY, 2021

M.Sc. (PHYSICS)

[Ruby and Aryan]

2021

DEPARTMENT OF APPLIED PHYSICS
DELHI TECHNOLOGICAL UNIVERSITY
(Formerly Delhi College of Engineering)
Bawana Road, Delhi-110042

CANDIDATE'S DECLARATION


We Ruby and Aryan, Roll No(s). 2K19/MSCPHY/22 and 2K19/MSCPHY/32 student(s) of M.Sc. (Physics), hereby declare that the project Dissertation titled “Photocatalytic and antibacterial activity of silver nanoparticles using green approach” which is submitted by us to the Department of Applied Physics, Delhi Technological University, Delhi in partial fulfilment of the requirement for the award of the degree of Master’s in Physics, is original and not copied from any source without proper citation. This work has not previously formed the basis for the award of any Degree, Diploma Associateship, Fellowship or other similar title or recognition.

Place: Delhi

Date: 29 May 2021



Ruby



Aryan

CANDIDATE'S DECLARATION

We Ruby (2K19/MSCPHY/22) and Aryan (2K19/MSCPHY/32), student(s) of M.Sc. (Physics), hereby declare that the project Dissertation titled "PHOTOCATYLTIC AND ANTIBACTERIAL ACTIVITY OF SILVER NANOPARTICLES SYNTHESIZED USING GREEN APPRAOCH" which is submitted to the Department of Applied Physics, Delhi Technological University, Delhi is an authentic record of our own, carried out during a period from August 2020 to May 2021, under the supervision of **Dr. Mohan Singh Mehata** is in partial fulfilment of the requirement for the award of the degree of Master's in Physics, is original and not copied from any source without proper citation. This matter presented in this report/thesis has not been submitted by us for the award of any Degree, Diploma Associateship, Fellowship or other similar title or recognition. This work has been published in SCI/SCI expanded/SSCI/Scopus journal OR peer reviewed Scopus indexed journal with following details:

Title of Paper: "Green synthesis of silver nanoparticles using *Kalanchoe pinnata* leaves (life plant) and their antibacterial and photocatalytic activity".

Authors names (in sequence as per research paper): Aryan, Ruby, Mohan Singh Mehata

Name of the journal: *Chemical Physics Letters* (Elsevier); **Impact Factor = 2.029**

Status of paper (Accepted/published/communicated): Published

Date of communication: 16th April 2021 **Date of acceptance:** 18th May 2021, **Date of publication:** 21st May 2021.

Name (Roll no): Ruby (2K19/MSCPHY/22), Aryan (2K19/MSCPHY/32)

SUPERVISOR CERTIFICATE

To the best of my knowledge, the above work has not been submitted in part or full for any Degree or Diploma to this university or elsewhere. I further certify that the publication and indexing information **given by student(s) is correct.**

Place: New Delhi
Date: 31st May 2021


31/5/2021

SUPERVISOR SIGN

NOTE: PLEASE ENCLOSE RESEARCH PAPER ACCEPTANCE/PUBLICATION/COMMUNICATION PROOF ALONG WITH SCOPUS INDEXING PROOF <https://doi.org/10.1016/j.cplett.2021.138760>

JOURNAL PROOF

CHEMICAL PHYSICS LETTERS

Publisher: ELSEVIER, RADARWEG 29, AMSTERDAM, NETHERLANDS, 1043 NX

ISSN / eISSN: 0009-2614 / 1873-4448

Web of Science Core Collection: Science Citation Index Expanded

Additional Web of Science Indexes: Current Contents Physical, Chemical & Earth Sciences | Essential Science Indicators

[Share This Journal](#)

[View profile page](#)

* Requires free login.



ELSEVIER

[About Elsevier](#)

[Products & Solutions](#)

[Services](#)

[Shop &](#)



[Visit journal homepage >](#)

[Submit your paper >](#)

[Open access options >](#)

[Guide for authors >](#)

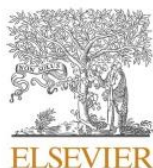
[Track your paper >](#)

[Order journal >](#)

[Browse journals >](#) [Chemical Physics Letters >](#) [Abstracting and Indexing](#)

Abstracting and Indexing

- [Chemical Abstracts](#)
- [Physics Abstracts](#)
- [Physikalische Berichte](#)
- [Current Contents - Physical, Chemical & Earth Sciences](#)
- [Nuclear Engineering Abstracts](#)
- [Scopus](#)
- [ISI Chemistry Reaction Center](#)
- [Science Citation Index](#)
- [Science Citation Index Expanded](#)
- [Current Chemical Reactions](#)
- [Reaction Citation Index](#)
- [INSPEC](#)



Research paper

Green synthesis of silver nanoparticles using *Kalanchoe pinnata* leaves (life plant) and their antibacterial and photocatalytic activities

Aryan¹, Ruby¹, Mohan Singh Mehata^{*}

Laser-Spectroscopy Laboratory, Department of Applied Physics, Delhi Technological University, Bawana Road, Delhi 110042, India



ARTICLE INFO

Keywords:

Silver nanoparticles
Kalanchoe pinnata
 Antibacterial activities
 Photocatalysts
 Surface plasmon resonance

ABSTRACT

Silver nanoparticles (AgNPs) were synthesized via green synthesis using a new herbal plant *Kalanchoe pinnata* (known as life plant) leaves. Effects of physicochemical parameters like temperature, pH and concentration on AgNPs were examined, and the absorption spectra were observed due to strong surface plasmon resonance. The crystalline nature and stability of AgNPs were confirmed by XRD pattern and zeta potential, respectively. The morphology of AgNPs was studied using FESEM and HRTEM. AgNPs showed antibacterial activity against the gram-negative *E. Coli* bacteria and photocatalytic activity in the degradation of rhodamine B dye with a reaction rate constant of 0.042 min^{-1} .

1. Introduction

Nowadays, nanotechnology plays a vital role in technology and development. There is increased progress in nanotechnology due to the small size (1–100 nm) and unique properties of metallic nanoparticles (NPs), having a higher surface-to-volume ratio, which differentiates them from their bulk properties [1,2]. Metal nanoparticles [3,4] are used in different branches of health and medicine [5,6], photonics [7], sensors [8], and catalyst [9]. The unique optical, electrical, chemical and physical properties depend on the morphology of nanoparticles [10,11], which are further used in various applications, mainly in drug delivery [12,13].

Silver nanoparticles (AgNPs) synthesis was carried out using chemical [14–16] and physical approaches like laser or UV-irradiation [17], microwave irradiation [18], electrochemical reduction [19] and thermal decomposition [20]. It has been found that chemical-based silver nanoparticles are expensive, require high energy consumption [21], and hazardous to animal cells, humans and the environment [22]. To overcome these effects, green synthesis is considered an effective way to reduce the production cost, energy efficiency [23–25], and reduce toxic chemical compounds [26–28]. AgNPs were bio-synthesized with different biomasses like plant extracts [29–32], bacteria, fungi [33,34], algae [35] and other microorganisms [36–38]. To vanquish complicated cell sculpture procedure, synthesis of AgNPs using aqueous leaves extract is preferred [23,27,39]. AgNPs are used in nanotechnology due

to their antioxidant [40–42] antiproliferative [43], antidiabetic [44], antimycotic [45] and anticancer [28,46] properties. AgNPs have good application in water treatment [47], sensors [10,48], treat infections in open wounds [49], mosquito larvicidal [50], and household appliances [51–53].

Various medical plants were used for the synthesis of AgNPs [54–56]. *Kalanchoe pinnata* (*Bryophyllum pinnatum*), commonly known as *patherchat* or *patharkuchi* is a medical plant that belongs to the family of *Crassulaceae* [57] and has been long used in ayurvedic medicine from ancient times. The plant grows in countries like India, Hawaii, Tropical Africa, and Australian continents. Different parts of the plant are used in treatment like stems, leaves, roots, and flowers. The plant leaves contain other properties like antiviral, antimicrobial, anti-inflammatory [58], antitumor, antidiabetic [59], antilithic [60,61], wound healing [62], which is due to the presence of molecular groups in the plant-like alkaloids, phenols and flavonoids, etc.

Dye released from major textile industries and other factories causes severe environmental problems [63,64]. Green technology plays a crucial role in solving this problem by reducing cost and is ecological [65–67]. Synthesized AgNPs are more reactive to the chemical compound because of a higher surface to volume ratio [68] and are used for dye degradation following a photocatalytic reduction under UV-irradiation [69,70]. Rhodamine B (RhB) is a harmful dye to humans, causing harm to the skin and itching in the eyes, and detrimental to aquatic life. Therefore, in the present study, we have used a specific

* Corresponding author.

E-mail address: mismehata@gmail.com (M.S. Mehata).¹ Both the authors contributed equally.

<https://doi.org/10.1016/j.cplett.2021.138760>

Received 16 April 2021; Received in revised form 16 May 2021; Accepted 18 May 2021

Available online 21 May 2021

0009-2614/© 2021 Elsevier B.V. All rights reserved.

PLAGRISM REPORT

5/31/2021

Project Thesis .docx



T2 Project Thesis .docx

May 31, 2021

9373 words / 52608 characters

Project Thesis .docx

Sources Overview

9%

OVERALL SIMILARITY

1	link.springer.com INTERNET	<1%
2	Aryan, Ruby, Mohan Singh Mehata. "Green synthesis of silver nanoparticles using Kalanchoe pinnata leaves (life plant) and their antiba- CROSSREF	<1%
3	www.tandfonline.com INTERNET	<1%
4	www.hindawi.com INTERNET	<1%
5	Tahir, Kamran, Sadia Nazir, Baoshan Li, Arif Ullah Khan, Zia Ul Haq Khan, Aftab Ahmad, and Faheem Ullah Khan. "An efficient photo cat- CROSSREF	<1%
6	www.nature.com INTERNET	<1%
7	Kalaivani Dayanidhi, Noorjahan Sheik Eusuff. "Distinctive detection of Fe and Fe by biosurfactant capped silver nanoparticles naked e- CROSSREF	<1%
8	Higher Education Commission Pakistan on 2018-04-08 SUBMITTED WORKS	<1%
9	University of Leeds on 2017-09-12 SUBMITTED WORKS	<1%
10	Siddhant Jain, Mohan Singh Mehata. "Medicinal Plant Leaf Extract and Pure Flavonoid Mediated Green Synthesis of Silver Nanoparticl- CROSSREF	<1%
11	Sneha, K. "Counter ions and temperature incorporated tailoring of biogenic gold nanoparticles", Process Biochemistry, 201009 CROSSREF	<1%
12	University of the Philippines - Manila on 2018-12-14 SUBMITTED WORKS	<1%
13	mafiadoc.com INTERNET	<1%
14	Manoj Kumar Choudhary, Jyoti Kataria, Shweta Sharma. "Evaluation of the kinetic and catalytic properties of biogenically synthesized ... CROSSREF	<1%
15	Savitribai Phule Pune University on 2018-07-06 SUBMITTED WORKS	<1%
16	Achyuta Kumar Biswal, Pramila Kumari Misra. "Biosynthesis and characterization of silver nanoparticles for prospective application in ... CROSSREF	<1%
17	Chandra Shekar Bhatt, Bharathkumar Nagaraj, Anil Kumar Suresh. "Nanoparticles-shape influenced high-efficient degradation of dyes: ... CROSSREF	<1%

<https://id.talimilarity.turnitin.com/viewer/submission/old/275357311372/print?locale=en>

1/50

5/31/2021		Project Thesis.docx	
42	lopscience.lap.org INTERNET	<1%	
43	www.degruyter.com INTERNET	<1%	
44	www.mdpi.com INTERNET	<1%	
45	Arpita Roy, Navneeta Bharadvaja. "Silver nanoparticle synthesis from and its dye degradation activity", Bioinspired, Biomimetic and N... CROSSREF	<1%	
46	Higher Education Commission Pakistan on 2015-06-23 SUBMITTED WORKS	<1%	
47	Fisseha A. Bezza, Shepherd M. Tichapondwa, Evans M.N. Chirwa. "Synthesis of biosurfactant stabilized silver nanoparticles, character... CROSSREF	<1%	
48	University of Iowa on 2015-12-09 SUBMITTED WORKS	<1%	
49	VIT University on 2019-06-19 SUBMITTED WORKS	<1%	
Excluded search repositories:			
• None			
Excluded from Similarity Report:			
• Bibliography			
Excluded sources:			
• None			



Ruby



Aryan



(Dr. Mohan Singh Mehata)


SUPERVISOR

ACKNOWLEDGEMENT

We would like to express our deepest sincere and gratitude to our supervisor, Dr. Mohan Singh Mehata, Assistant Professor, Department of Applied Physics, Delhi Technological University for giving us the opportunity to work under his guidance and for constant inspiration and incessant support throughout the project. We take this opportunity to express our indebtedness to our supervisor for his enthusiastic help, his expertise, brilliant ideas, valuable suggestions and constant encouragement. We are grateful to acknowledge the constant help and convenience at every step of our project by all the lab members (PhD scholars), Dept. of Applied Physics. Lately, we are thankful to our families and friends for their love, care and support who patiently extended all sorts of help for accomplishing this task.

A rectangular box containing a handwritten signature in blue ink that reads "Ruby".

Ruby

A rectangular box containing a handwritten signature in blue ink that reads "Aryan".

Aryan

ABSTRACT

Green synthesis is a novel way to synthesizing nanoparticles by using different biological masses. Silver nanoparticles (AgNPs) were synthesized via green synthesis using new and different herbal plant like *Kalanchoe pinnata* and *Abutilon theophrasti* leaves. The variation of physical parameters like temperature, pH, and concentration on the emergence and stability of nanoparticles was examined. The absorption of synthesized AgNPs was observed due to the strong surface plasmon resonance (SPR), whereas the crystalline nature was confirmed by XRD pattern. The morphology of AgNPs was studied using FESEM and HRTEM. Zeta potential strongly supported the high stability of silver nanoparticles. AgNPs showed antibacterial activities against the gram-negative *E. Coli* bacteria. Synthesised AgNPs showed the excellent photocatalytic activity in wastage water treatment in different Dye degradation.

CONTENTS

Cover page	i	
Declaration	ii	
Certificate	iii	
Journal proof	iv-v	
Plagiarism	vi-vii	
Acknowledgement	viii	
Abstract	ix	
Contents	x	
List of Figures	xiii	
List of Tables	xv	
List of Symbols and abbreviations	xvi	
CHAPTER 1	INTRODUCTION	1-7
1.1	Introduction	
1.2	Literature review	
	1.2.1.1.1	Metallic nanoparticles
1.3	Methods for nanoparticles synthesis	
	1.3.1.1.1	Physical method
	1.3.1.1.2	Chemical method
	1.3.1.1.3	Biological method
1.4	Description of plants	
1.5	Properties of Silver nanoparticles	
1.6	Antibacterial activity of AgNPs	
1.7	Photocatalytic activity of AgNPs in dye degradation	

1.8	Aim and scope of study	
CHAPTER 2	MATERIALS AND METHOD	8-10
2.1	Materials used	
2.2	Leaves used	
	2.2.1 <i>Kalanchoe pinnata</i> extract	
	2.2.2 <i>Abutilon theophrasti</i> extract	
2.3	Silver nanoparticle synthesis	
2.4	Sample for catalysis	
	2.4.1 For RhB dye	
	2.4.2 For MO dye	
CHAPTER 3	CHARACTERIZATION TECHNIQUES	11-13
3.1	UV/VIS/NIR spectroscopy	
3.2	X-ray diffraction	
3.3	FESEM and HRTEM	
3.4	Zeta potential	
CHAPTER 4	RESULT AND DISCUSSIONS	14- 32
4.1	Effect of silver salt and plant extract concentration on AgNPs emergence (<i>Kalanchoe pinnata</i>)	
4.2	AgNPs formation at different reaction times	
	4.2.1 Using <i>Kalanchoe pinnata</i>	
	4.2.2 Using <i>Abutilon theophrasti</i>	
4.3	Effect of pH on AgNPs formation	
	4.3.1 Using <i>Kalanchoe pinnata</i>	
	4.3.2 Using <i>Abutilon theophrasti</i>	
4.4	AgNPs formation at different reaction temperature	
	4.4.1 Using <i>Kalanchoe pinnata</i>	
	4.4.2 Using <i>Abutilon theophrasti</i>	

- 4.5 XRD pattern of AgNPs
 - 4.5.1 Using *Kalanchoe pinnata*
 - 4.5.2 Using *Abutilon theophrasti*
- 4.6 AgNPs morphology
- 4.7 Zeta potential for silver nanoparticles
 - 4.7.1 Using *Kalanchoe pinnata*
 - 4.7.2 Using *Abutilon theophrasti*
- 4.8 AgNPs catalytic activity
 - 4.8.1 RhB degradation under UV irradiation
 - 4.8.2 MO degradation under Sunlight
- 4.9 Antibacterial activity of AgNPs

CHAPTER 5	CONCLUSION	33
APPENDIECES		34-35
REFERENCES		37-46
RESEARCH PAPER		47-55

LIST OF FIGURES

- Figure 1.1** Biomasses used in Biological synthesis
- Figure 2.1** Diagrammatical representation of synthesised AgNPs using *Bryophyllum pinnatum* (a) and *Abutilon theophrasti* (b)
- Figure 3.1** Perkin Elmer Lambda 750 spectrometer
- Figure 3.2** BRUKER-D8 advanced to record XRD pattern
- Figure 3.3** JEOL JSM-7610F Plus for FESEM
- Figure 3.5** HRTEM using TALOS
- Figure 3.6** Malvern Panalytical Zetasizer (Nano Series ZS).
- Figure 4.1** The absorption spectra of leaves extract, silver salt, and AgNPs synthesized using *Kalanchoe pinnata* (a) and *Abutilon theophrasti* (b) leaves extract in an aqueous medium.
- Figure 4.2** The absorption spectra of AgNPs at various silver salt concentrations (a) and with varying ratios of plant extract concentrations (b). Inset of (a) demonstrated the shift in band maximum with the concentration of silver salt at a constant amount of plant extract and (b) the absorption spectrum of plant extract.
- Figure 4.3** The color of the *Kalanchoe pinnata* leaves extract, silver salt, and formation of AgNPs in the water with reaction time (a) and the absorption spectra of AgNPs at various reaction time intervals (b). Inset of (b) shows the increase in absorption intensity with reaction time.
- Figure 4.4** Color change in silver salt plant extract solution with time (a) and absorption spectra of AgNPs at various reaction time intervals. Inset (b) shows the shift in peak of absorption maximum as a function of time.
- Figure 4.5** The absorption spectra of AgNPs in the water at various pH using *Kalanchoe pinnata* (a) and *Abutilon theophrasti* (b) leaves. Inset shows the shift in band maximum as a function of pH.

- Figure 4.6** The absorption spectra of AgNPs in water at various temperatures using *Kalanchoe pinnata* (a) and *Abutilon theophrasti* (b) leaves. Inset shows the shift in band maximum as a function of temperature.
- Figure 4.7** X-ray diffraction pattern of synthesized AgNPs using *Kalanchoe pinnata* (a) and *Abutilon theophrasti* (b) leaves.
- Figure 4.8** FESEM images of AgNPs thin film synthesized using *Kalanchoe pinnata* leaves.
- Figure 4.9** HRTEM images of AgNPs synthesized using *Kalanchoe pinnata* leaves extract at different magnifications.
- Figure 4.10** Particle size distribution for AgNPs synthesized using *Kalanchoe pinnata* (a) and *Abutilon theophrasti* (b) leaves extract.
- Figure 4.11** Change in colour of RhB dye (10 μM) dissolved in water in the presence of AgNPs with doses of UV-light irradiations.
- Figure 4.12** The absorption spectra of RhB dye in water in the presence of AgNPs at different time intervals in the dark.
- Figure 4.13** The absorption spectra of RhB dye in water in the presence of AgNPs at different time intervals under UV irradiation.
- Figure 4.14** Plots of C/C_0 against reaction time for reducing RhB dye in the presence of AgNPs in the dark and under UV light.
- Figure 4.15** Change in color of the dye MO, after degradation under sunlight (a) and dark conditions (b).
- Figure 4.16** Absorption spectra of MO dye solution in water at different reaction times in the presence of AgNPs under dark conditions (a) and sunlight (b).
- Figure 4.17** Plots of $\ln(C_t/C_0)$ against reaction time for reducing MO dye in the presence of AgNPs in the dark and under sunlight.
- Figure 4.18** Zone of inhibition of *E-coli* bacteria treated with *Kalanchoe pinnata* leaves extract (a), silver nitrate (b), and AgNPs (c).

LIST OF TABLES

Table 1. EDX analysis parameters of AgNPs recorded in thin-film.

Table 2. Zone of inhibition for plant extract, AgNO₃ and AgNPs treated with *E. coli* bacterial strain.

LIST OF SYMBOLES AND ABBREVIATIONS

MIT	Massachusetts Institute of Technology
NMs	Nanoparticles
NPs	Nanoparticles
AgNPs	Silver nanoparticles
LSPR	Localized Surface Plasma Resonance
RhB	Rhodamine Blue
MO	Methyl Orange
DNA	Deoxyribonucleic acid
MRI	Magnetic Resonance Imaging
WHO	World Health Organisation
AgNO ₃	Silver Nitrate
UV-Vis	Ultraviolet-Visible
FWHM	Full Width Half Maxima
SEM	Scanning Electron Microscopy
SPR	Surface Plasma Resonance
TEM	Transmission Electron Microscopy
EDX	Energy Dispersive Spectroscopy
NIR	Near Infrared Spectroscopy
DLS	Dynamic Light Scattering

SA: V

Surface area to volume ratio

XRD

X-Ray Diffractometer

CHAPTER 1

INTRODUCTION

1.1 INTRODUCTION

In materials science, Nanotechnology is the most growing and active research area. The idea of modern nanotechnology originated from Richard Feynman, a Nobel Laureate in Physics in 1959. This concept was initially introduced during a lecture titled “There’s Plenty of Room at the Bottom” presented by Richard Feynman introducing the matter at atomic level. The following idea originates new ways of thinking and exploring the matter at atomic level. That’s why he is considered as the father of modern Technology [1]. Nanomaterials have been long used by Indian medicine System even before term “nano” introduced [2].

Nano is most fascinating area of research with incredible applications in different parts of science and medicine [3]. The development in altering and exploring properties of nanomaterials by changing their shape and morphology. In recent years impressive development in fabrication, synthesis and methodologies of nanomaterials. This field is emerging day by day rapidly. Nanoparticles plays a very vital role in nanotechnology [4]. Nanoscience has successfully created nanomaterials (NMs) with size less than or equal to 100 nm [5]. They exhibit novel and improved mechanical, optical and electronic properties because of its very small size [6], [7]. Many inert metals like silver also distinctive properties when it is downsized to the nanoscale [8].

1.2 LITERATURE REVIEW

1.2.1 Metallic nanoparticles

Nanotechnology can be subdivision of science and engineering keen to materials. Nano-science deals with the study of the phenomena at 1-100 nm particle size and nanomaterials ranging one dimension less than 100 nm [9]. Since the past decade a separate class of materials derived from nanomaterials as nanoparticles. Most fascinating are metal nanoparticles. Due to their high conductivity, they have received a great scientific interest as compared to metal oxides nanoparticles. Metal-metal chemical bond is not represented in metal nanoparticles and it isolated particles between 1-100 nm size. Metal nanoparticles (NPs) have extraordinary

different properties as compared to their bulk metal that mostly contains a degenerated density of energy states and a large surface-volume ratio along with nm scale sizes. Therefore, they show high chemical activity and specificity as compared to bulk metals so that they are attractive to use as catalysts. The high SA:V along with size effects gives metal nanoparticles distinctively unique properties from those of bulk metal [10].

In past two decades, nanoparticles exhibit many fascinating applications in variety fields like conductors, electronics, sensors, medicine, catalysis, optical and biological devices etc [11], [12] because of their unique properties, which vary from molecular or bulk materials. Researchers also have achieved decent awareness in nanomaterials due to their applications in medicine and unique properties [13]. AgNPs properties depends on the distinct shape and nanoparticle size, surrounding media, and their fabrication method [14]. So, Researchers and Scientists are more interested in targeting fabrication of metal nanoparticles. Desired shape and size of MNs allow exploring its applications in various fields.

1.3 METHODS FOR NANOPARTICLES SYNTHESIS

The top-down synthesis method of NMs initiates from a suitable starting material via sputtering, mechanical grinding etc. while second method synthesis smaller entities such as atoms and molecules are joined with each other and fabricated into NMs with processes like chemical methods and biological methods [15]. The small particles form a complex cluster by oxidation/reduction, nucleation and growth processes. Imperfections are introduced by a top-down so, bottom-up approach is most preferable approach for synthesis. NMs properties also depends on synthesis methods [16].

1.3.1 Physical Methods

These methods include evaporation of the material followed by controlled condensation, pyrolysis and laser ablation. In this method nanoparticles are critically affected by parameters like time of drilling, medium and initial method [14]. It is typical representation of top-down method [17]. This method is restricted to presence of chemical agents in the solution for AgNPs production. This method advantages are, uniform NPs distribution and no solvent contamination in thin films. Its main limitations are expensive equipment and lower production rate compared to chemical methods. The additional handicap includes the high energy consumptions.

1.3.2 Chemical Methods

The second route consists of sol-gel technique which is used to synthesis nanoparticles in liquid phase or colloidal solution. this method is a representation of bottom-up approach [18]. This process contains nanomaterials as subclass of colloids, which has dimensions in the nano range. The formed nanomaterials may be nanoparticles, fibres or nanoplates. The main advantage of this method are simple technique, low temperature synthesis, formation of variety particles in terms of shape and size, large quantities can be produced [19]. However, it has some disadvantages including toxic chemicals and hazardous reaction by-products.

1.3.3 Biological Synthesis

Green synthesis is becoming an emerging route actively participating in the progress in the fields of science & industry [20]. Living cells are very complicated systems with hundreds of molecules containing various functional groups which easily helps in reduction of metal ions.

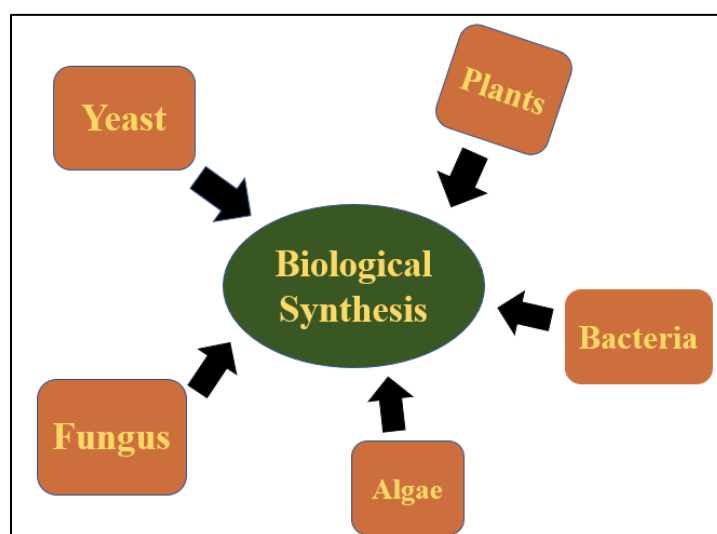


Figure 1.1. Different biomasses used in Biological synthesis

Therefore, this method need more research to elaborate a specific process directly reasonable for growth of nanoparticles. So, biological organisms such as microorganism [21], plant extracts and biomasses can be good option for nanoparticles synthesis. It is simple, inexpensive, economic, environmentally friendly and toxic free [22]. This method is like a revolution in nanoparticles's world [12].

Researchers in biological systems increased due to its excellent features in a variety of organisms in our eco-system like viruses, bacteria, yeast, fungi [23] and different parts of plants

[24] have ability to form inorganic materials [25]. It is a non-toxic, high yield, fast, energy saving process among the other methods. Many microorganisms were frequently used in nanoparticles fabrication [26]. Both unicellular and multicellular organism produce metallic NPs but separation of tiny produced particles from cell debris is complicated and the capping and matrix proteins can influence the properties of NPs. The plant parts are mainly in sundried form and considered as a best solution to above problems for NPs synthesis.

The plant extract contains all the necessary chemical constituents like reducing and stabilizing agent. A plant leaves is a mixture of complex structures, each compound can perform multiple roles, acting as green chemical agents. The use of single multifunctional agent is always more advantageous and easier to deal from unwanted toxic parts during synthesis process. The main advantage of plants over microorganisms is that they are easily available and don't need any special conditions for storage and care as needed in the case of microorganisms.

1.4 DESCRIPTION OF PLANTS

India has a rich diversity of plants with different and unique medicinal properties. In present study mainly two plants leave *Kalanchoe pinnata* and *Abutilon theophrasti* were used in the AgNPs synthesis [27]–[29]. *Kalanchoe pinnata* (*Bryophyllum pinnatum*), commonly known as *patherchat* or *patharkuchi* is a medical plant that belongs to *Crassulaceae* family [30] and used in ayurvedic medicine from ancient times. The plant grows in countries like India, Hawaii, Tropical Africa, and Australian continents. Different parts of the plant are used in treatment like stems, leaves, roots, and flowers. The plant leaves contain other properties like antiviral, antimicrobial, anti-inflammatory [31], antitumor, antidiabetic [32], antilithic [33], [34], wound healing [35], which is because of molecular groups present in plant-like alkaloids, phenols and flavonoids, etc. Using the green synthesis method, AgNPs can be synthesized using various entities like plants [36]–[40], microorganisms [26], and enzymes [25]. Silver shows antimicrobial and catalytic properties [41], synthesized AgNPs enhances those properties to a higher extent making AgNPs very practical and valuable in the medical field and wastewater management [42]–[45]. Current study includes AgNPs synthesis with help of plant leaves of *Abutilon theophrasti*. It is an ethnomedicinal weed plant mainly cultivated for oil and fibre [46]. The leaves, stem, roots, and seeds of the plant exhibit properties like anti-inflammatory, carminative, etc., used to treat rheumatic pains, sprains and dysentery [47].

1.5 SILVER NANOPARTICLES PROPERTIES (AgNPs)

Various properties of AgNPs are:

- Surface area to volume ratio:

It has a significant effect on the nanoparticle properties. If they have a large surface area per unit volume then they are more chemically reactive related with the bigger particles. Materials are found to be inert in bulk form and are reactive when change into nanoscale form.

- Optical and electronic properties

These properties are interconnected as the incident photons interact with electrons and show collective excitations, this is known as localized surface plasma resonance (LSPR) [48].

The peak wavelength of the LSPR spectrum is dependent upon the interparticle spacing, size and shape of the nanoparticles. These electronic and optical properties of nanoparticles are very useful in optical filters and sensors.

- Magnetic properties

This property is depending on the uneven electronic distribution of nanoparticles. They are used in wide range of disciplines, such as homogenous catalysis, heterogeneous, biomedicine, magnetic fluids, data storage magnetic resonance imaging (MRI).

- Quantum confinement effect

This property of nanoparticles is used in several technologies such as sensors, memory applications and electronics etc. The quantum confinement effect is analysed when the size of the particle is too short to be coordinate to the wavelength of the electron.

1.6 ANTIBACTERIAL ACTIVITY OF AgNPs

The proper mechanism of antimicrobial effect of AgNPs on bacteria is a topic of debate [49]. Various different theories are given explaining AgNPs action on bacteria causing antibacterial effect. When AgNPs penetrates cell, they have the ability to alter the physiochemical properties by interacting with the cellular structure and cell's biomolecules, changing cell's structure and causing malfunctioning in normal physiological properties such as respiration and permeability of the cell. Further, AgNPs interact with biomolecules of cells forming various oxygen and nitro species that cause stress in the cell's DNA and eventually leading to cell's death [49,50].

The particles can also destroy the DNA by acting on the soft bases, due to which cell dies. The nanoparticles can modulate the signal transduction in bacteria. Phosphorylation of protein substrates in bacteria is a well-established fact that influences bacterial signal transduction. But it not sufficient to understand and to establish the claims. Inorganic nanomaterials studied in current researches shown the superior antimicrobial activity which extended its medicinal use. [51]. Silver is a good metal of choice to kill microbes efficiently. Silver nanoparticles is a growing field in with promising antibacterial activity recently known that acts on both extracellularly as well as intracellularly.

1.7 PHOTOCATALYTIC ACTIVITY OF AgNPs IN DYE DEGRADATION

The textile dyeing industry has generated massive pollution problem as it is chemically intensive industries with number one pollutant of water. Only 80 percent of the dyestuffs stay on the fabric and rest go down the trench. The liberation of waste waters having harmful dyes is the reason for serious damage to aquatic life, directly by photosynthesis and oxygenation. these compounds are toxic and discard to natural degradation like light, acid, base and oxygen due to this the color of the dye becomes permanent. Azo dyes in majority are water-soluble and body can easily absorb them through inhalation, skin contact and swallowing due to this these dyes are the cause of mutagen and cancer. Azo dyes are harmful to aquatic environment [52,53]. Green technology plays a crucial role in solving this problem by reducing cost and is ecological [54]–[56]. Synthesized AgNPs are more reactive to the chemical compound because of a higher surface-volume ratio [57] so, used in dye degradation following a photocatalytic reduction under UV-irradiation [58,59]. Rhodamine B (RhB) is a harmful dye to humans, causing harm to the skin and itching in the eyes, and detrimental to aquatic life.

The oxidative reduction technique is an effective method in degradation of such harmful dyes [60]. Nanomaterials like TiO₂ require UV light for their activation [61]; however, AgNPs exhibit strong absorption under natural light, and their high reactivity and selectivity enhance their photocatalytic activity [62]. In recent studies, photocatalytic degradation of MO is done using AgNPs [59]. Therefore, in the present study, we have used a specific plant (*Kalanchoe pinnata*, *Abutilon theophrasti*) leaves extract to synthesize AgNPs at various physicochemical parameters. The developed AgNPs were used to degrade industrial dye, RhB under UV-irradiation and antibacterial activities against gram-negative bacterial strain and further, AgNPs were used to degrade MO dye which can be further used for water treatment.

1.8 AIM AND SCOPE OF STUDY

- Eco-friendly biosynthesis of AgNPs using plant leaves extract controlled by physicochemical parameters.
- Analysing the morphology of the developed AgNPs by different characterization techniques.
- Examining remarkable antimicrobial properties of the Synthesized nanoparticles against *E. coli* gram-negative bacterial strains.
- Investigating the photocatalytic behaviour of AgNPs in Dye degradation.

CHAPTER 2

MATERIALS AND METHODS

2.1 CHEMICALS

Silver nitrate and sodium hydroxide were procured from Aldrich Chem. Co. and the obtained chemicals were utilized without further processing. 8.5 mg of Silver salt (AgNO_3) is mixed in 50 mL of ultrapure (UP) water to make 1 mM salt solution. For 2 mM, 3mM and, 4 mM the salt added is 17, 25.5 and 34 mg respectively. For 0.1 M sodium hydroxide (NaOH), 40 mg was added in 100 mL UP water.

2.2 LEAF EXTRACT

2.2.1 *Kalanchoe pinnata* extract

Fresh green *Kalanchoe pinnata* (*Bryophyllum pinnatum*) leaves were obtained from the DTU campus. To remove visible dust and impurity leaves were washed from tap water and later with UP water. Leaves of *Kalanchoe pinnata* were oven dried and crushed in powder form and 2 g of it was boiled in 50 mL UP water.

2.2.2 *Abutilon theophrasti* extract

Fresh *Abutilon theophrasti* leaves were obtained from the DTU campus. To remove visible dust and impurity leaves were washed from tap water and later with UP water. 5 g *Abutilon theophrasti* leaves were chopped and boiled in 50 mL UP water. Whatman filter paper is used for filtration and stored in refrigerator.

2.3 AgNPs SYNTHESIS

45 mL AgNO_3 was stirred and 5 mL extract solution was dropped wise using burette. The reaction temperature for *Kalanchoe pinnata* was kept at 60 °C and for *Abutilon theophrasti* the reaction take place at room temperature. For different concentration of silver salt and plant ratio similar process was repeated. Fig. 2.1 represents the schematic diagram of AgNPs synthesis.

2.4 SAMPLE FOR CATALYSIS

2.4.1 For RhB dye

4.8 mg of RhB ($C_{28}H_{31}ClN_2O_3$) dye was added in 10 mL of UP water to make a 10 μ M solution. 5 ml synthesised AgNPs (*Kalanchoe pinnata*) were mixed with 25 mL of RhB dye solution and stirred for the next 5 min to achieve an equilibrium state.

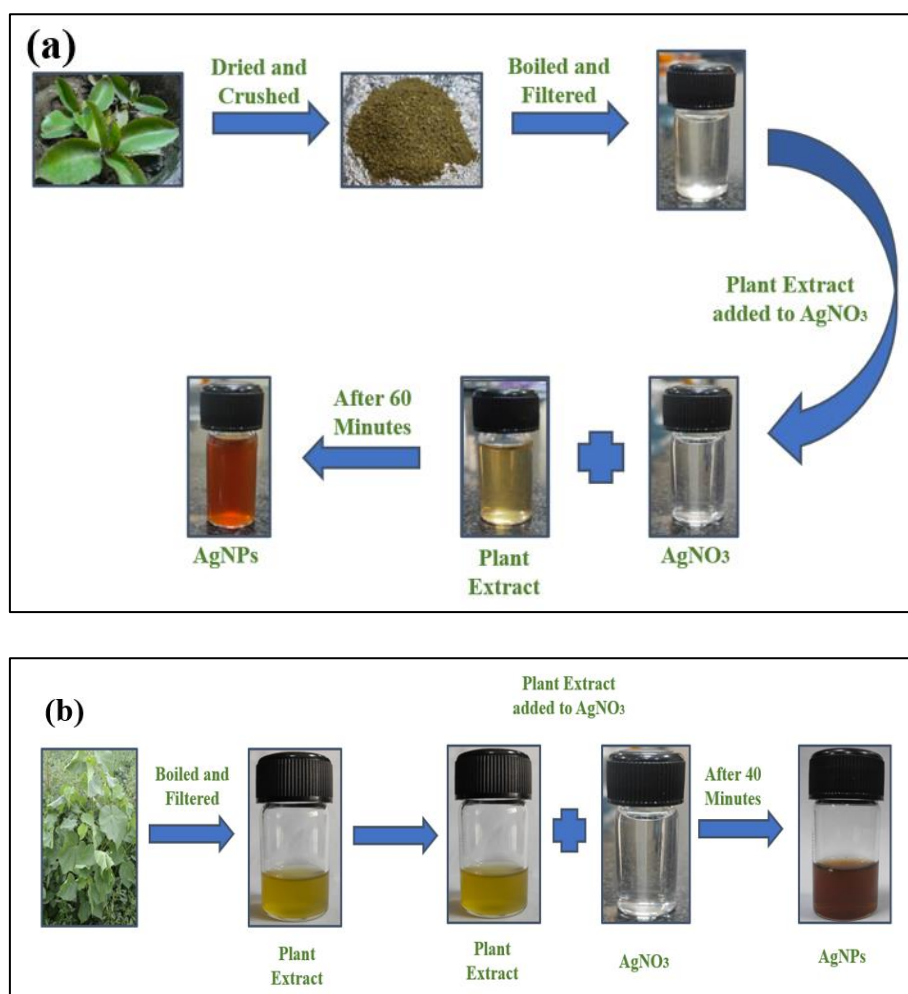


Figure 2.1. Diagrammatical representation of synthesised AgNPs using *Kalanchoe pinnata* (a) and *Abutilon theophrasti* (b)

The dye solution was then transferred into two glass vials, and one of them is stored in a dark room and another is illuminated using UV-light of 8 W and 254 nm (1.2 mW cm^{-2})

2.4.2 For MO dye

3.7 mg of MO ($C_{14}H_{14}N_3NaO_3S$) is added in 100 mL UP water to make a 100 μ M concentration solution. 5 mL synthesised AgNPs (*Abutilon theophrasti*) were mixed with 45 mL MO solution

and stirred for 30 min till equilibrium state achieved, later solution is transferred into two vials stored in dark and under natural light (sunlight).

CHAPTER 3

CHARACTERIZATION TECHNIQUES

3.1 UV/VIS/NIR SPECTROSCOPY

AgNPs absorption spectra were recorded using Perkin Elmer Lambda 750 spectrometer shown in Fig. 3. The observations were taken in the range 250 nm to 800 nm.

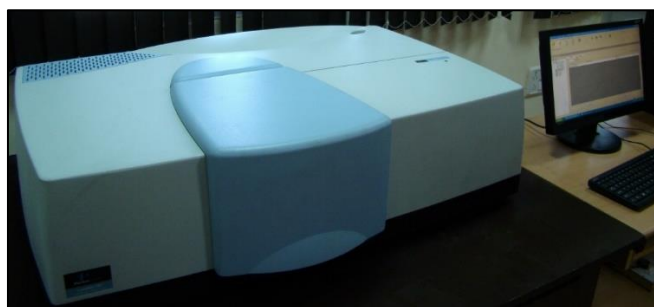


Figure 3.1 Perkin Elmer Lambda 750 spectrometer

3.2 X-RAY DIFFRACTION

XRD pattern for thin film was recorded by BRUKER-D8 advanced. Fig. 3.2 shows the XRD machine. The particle size is estimated using Scherer's relation $D = 0.9 \lambda / \beta \cos\theta$ corresponding to (111) peak. Here, D , λ and β represents particle size, wavelength and FWHM (full width at half maximum) and θ represents Bragg's angle.

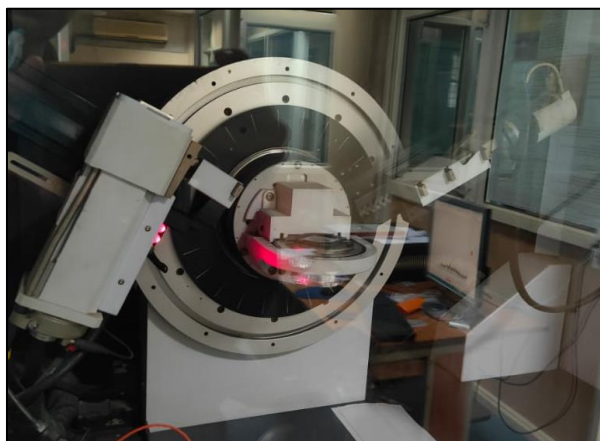


Figure 3.2 BRUKER-D8 advanced to record XRD pattern.

3.3 FESEM AND HRTEM

AgNPs shape and size was calculated using FESEM AND HRTEM. FESEM analysis was done using JEOL JSM-7610F Plus and HRTEM using TALOS accelerating at a voltage of 200 kV. Images of both instruments are shown in Figs. (3.3, 3.4)



Figure 3.3 JEOL JSM-7610F Plus for FESEM



Figure 3.4 HRTEM using TALOS

3.4 ZETA POTENTIAL

The size and zeta potential value of synthesised AgNPs in colloidal solution is analysed using Malvern Panalytical Zetasizer (Nano series ZS). Fig. 3.5 shows the device used for analysis



Figure 3.5 Malvern Panalytical Zetasizer (Nano series ZS).

CHAPTER 4

RESULT AND DISCUSSION

AgNPs emergence and morphology of AgNPs synthesized by *Kalanchoe pinnata* (*Bryophyllum pinnatum*) depend on environmental factors like reaction time, temperature, pH, concentration, etc. AgNPs, plant extract and silver salt absorption spectra for both plants is shown in Fig 4.1(a, b). A strong band observed at around 430 nm corresponds to the strong SPR of AgNPs.

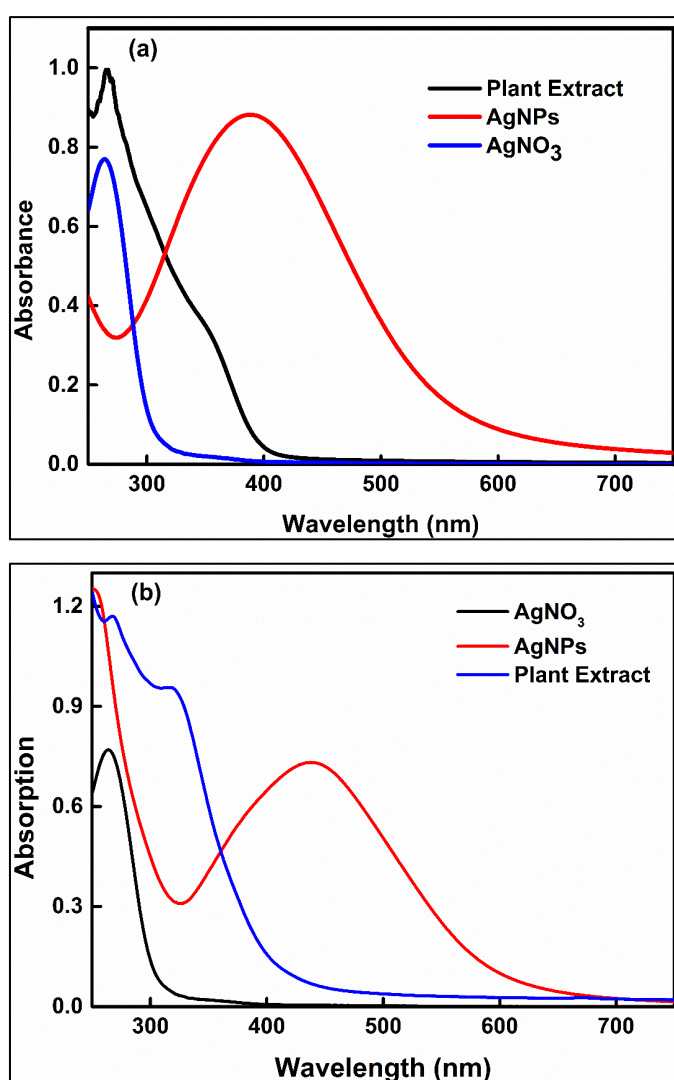


Figure 4.1. Absorption spectra of leaves extract, silver salt, and AgNPs synthesized using *Kalanchoe pinnata* (a) and *Abutilon theophrasti* (b) leaves extract in an aqueous medium.

4.1 EFFECT OF SILVER SALT AND PLANT LREAF EXTRACT CONCENTRATIONS ON AgNPs EMERGENCE

The emergence of AgNPs was studied at different silver salt concentrations and plant extract ratio as shown in Fig. 4.2(a, b). With the increase of the emergence rate of AgNPs, aggregation of nanoparticles was also increased with time, particularly at a higher concentration of precursor salt; hence optimization of concentration is also essential.

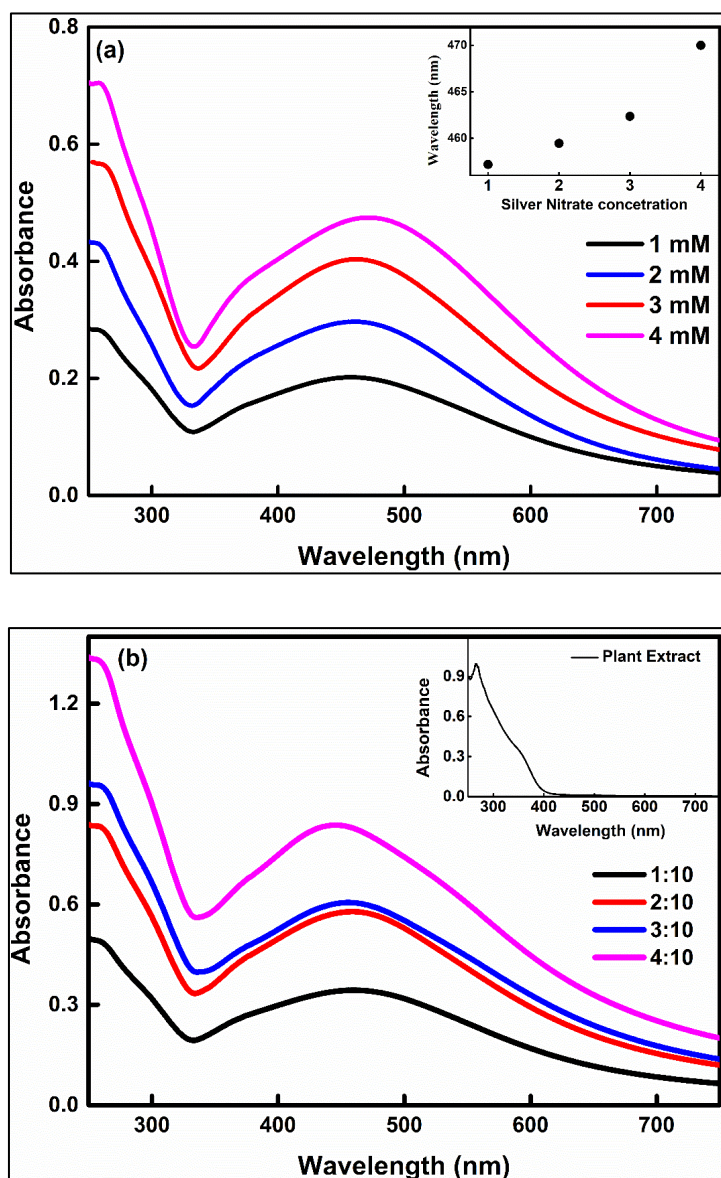


Figure 4.2. The absorption spectra of AgNPs at various silver salt concentrations (a) and with varying ratios of plant extract concentrations (b). Inset of (a) demonstrated the shift in band maximum with the concentration of silver salt at a constant amount of plant extract and (b) the absorption spectrum of plant extract.

4.2 AgNPs FORMATION AT DIFFERENT REACTION TIMES

4.2.1 Using *Kalanchoe pinnata*

When extract was mixed with 1 mM silver salt solution, solution colour initially changes pale yellow to dark brown, shown in Fig. 10(a). Solution colour change indicates AgNPs formation [63]. The plant leaves contain many bio-molecule such as flavonoids, phenols, quinines, etc., which acting as reducing and capping agents. They are accountable in reduction of Ag^+ to Ag^0 NPs. Solution's maximum colour change occurs within 60 min and no further change in color observed even after 24 h, suggests AgNPs stability. Synthesized AgNPs (*Bryophyllum pinnatum*) absorption spectra are shown in Fig. 10(b). Thus, the AgNPs absorption maximum lies between 420-450 nm and a rise in intensity suggests an enrichment in the AgNPs formation with time.

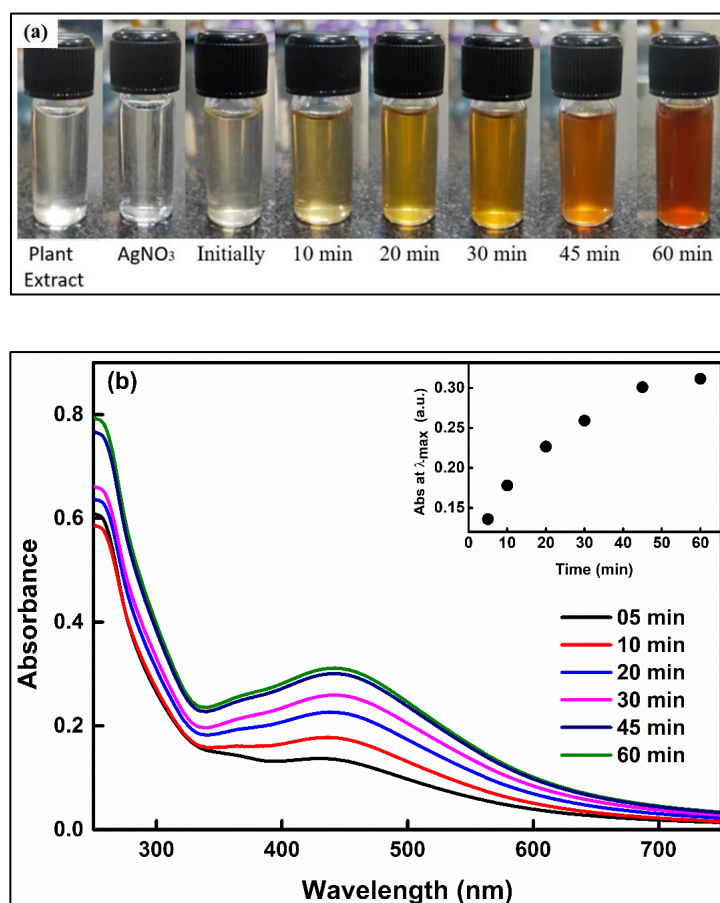


Figure 4.3. The color of the *Kalanchoe pinnata* leaves extract, silver salt, and formation of AgNPs in water with reaction time (a) and the absorption spectra of AgNPs at various reaction time intervals (b). Inset of (b) shows the increase in absorption intensity with reaction time.

4.2.2 Using *Abutilon theophrasti*

AgNPs emergence is first confirmed by observing color change at different reaction time, 5 mL extract was dropped in 45 mL silver salt. With time solution's colour was changed from pale yellow to dark brown suggesting AgNPs emergence, shown in Fig. 4.4(a) [12]. AgNPs formation initiated after 5 min and vigorously increases up to 40 min. The flavonoids and teraponids present in plant cause Ag^+ reduction to AgNPs [64]. Over time, a sharp SPR band was observed, and the peak intensity also increases with time [65]. Fig. 11(b) show absorption maximum peak at 439 nm.

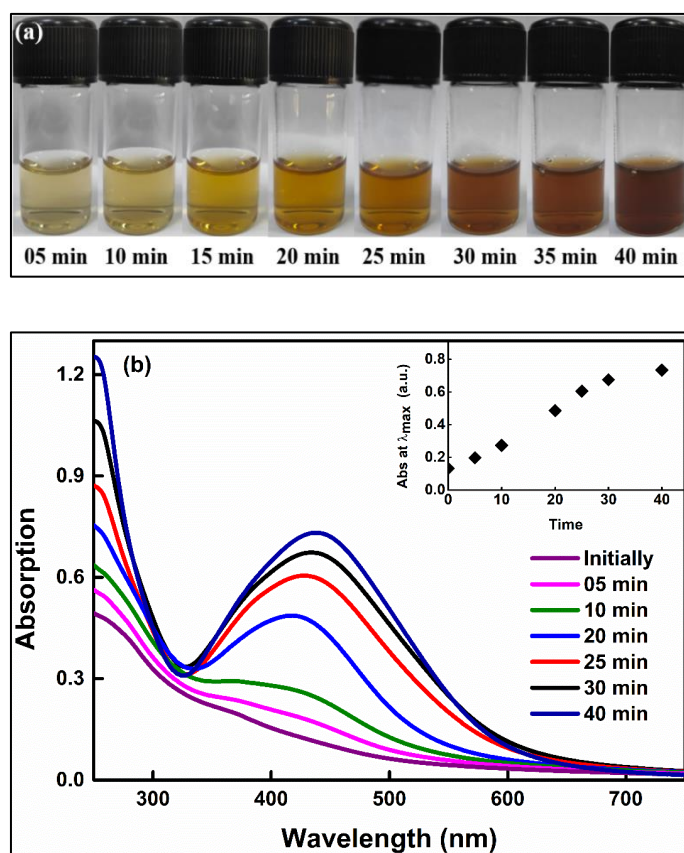


Figure 4.4. Color change in silver salt plant extract solution with time (a) and absorption spectra of AgNPs at various reaction time intervals. Inset (b) shows the shift in peak of absorption maximum as a function of time.

4.3 EFFECT OF pH ON AgNPs FORMATION

4.3.1 Using *Kalanchoe pinnata*

pH plays key part in changing shape, size, stability and AgNPs morphology [66,67]. In some cases, with the increase in pH, the particle size decrease [68]. While in other cases, the size of

AgNPs increases with increasing pH, this is due to higher accumulation at lower pH (< 5) and lower accumulation at higher pH (6 to 12). This happens because of functional groups present in different plants for nucleation [69]. Biomolecules have some electrical charges that were changed with a change in pH, which might change the properties of capping and stabilizing agents [70]. At different pH AgNPs absorption spectra is shown in Fig.4.5(a), indicating increase in absorption intensity with rising pH. At pH 5, absorption maximum is at 424 nm, with increasing pH from 5-12, SPR peak shifted from 420 to 440 nm, resulting in increase of the size of AgNPs due to a change in the net charge of biomolecules from positive to negative, initiating intense repulsion between the negatively charged ions. The results (Fig. 4.6 (a)) indicate that basic pH is further suitable for AgNPs synthesis [12].

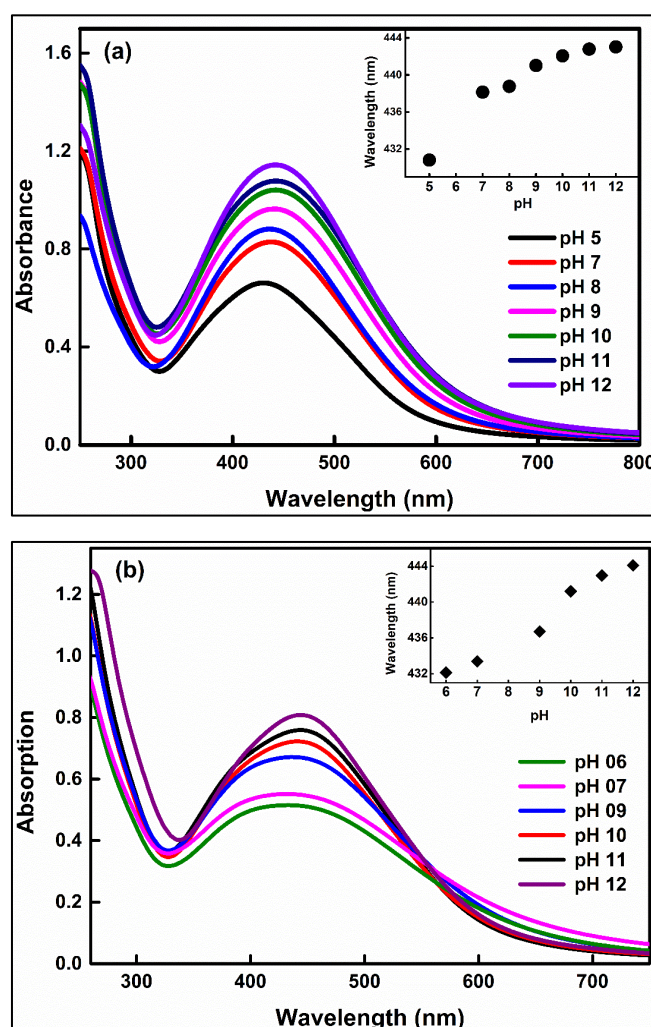


Figure 4.5. Absorption spectra of AgNPs in water at various pH using *Kalanchoe pinnata* (a) and *Abutilon theophrasti* (b) leaves. Inset shows the shift in band maximum as a function of pH.

4.3.2 Using *Abutilon theophrasti*

At a highly acidic pH, the biomolecules present in the extract are inactivated and lead to no absorption peak [71]. At very high basic pH, silver nanoparticles agglomerates and were unstable [72]. Therefore, the absorption spectrum of AgNPs was recorded for pH between 6-12 pH shown in Fig. 12 (b). SPR peak at pH 6 is at 432 nm having an intensity/absorbance of 0.5. On rising pH from 6 to 12, the SPR peak shifts to 444 nm, and the intensity increases to 0.8, a similar effect was observed in the previous study [73]. The results indicate that basic pH is further suitable for AgNPs synthesis.

4.4 AgNPs formation at different reaction temperatures

4.4.1 Using *Kalanchoe pinnata*

Temperature is a very prominent parameter for determining the morphology of synthesized AgNPs [74]. Fig. 13 (a) shows AgNPs absorption spectra at 10 °C to 60 °C in the interval of 10 °C. With the rise in temperature, the reaction rate increases, designate AgNPs emergence due to the increase in the reduction of Ag^+ into Ag^0 [75]. With the increasing temperature, the band maximum shows a blue shift from 440-420 nm due to localization of SPR. It implies AgNPs size decreases with a rise in temperature. With increasing the temperature, the molecules present in the extract solution get higher kinetic energy, resulting in a faster reduction process, indicating no further growth in the size of NPs. Thus, at higher temperatures, small particles with uniform size distribution were formed [20].

4.4.2 Using *Abutilon theophrasti*

Temperature is a dominating parameter responsible for shape, size, and AgNPs morphology. Fig. 13 (b) shows temperature effect in the range 10 °C to 60 °C on silver nanoparticle synthesis. With temperature increase, SPR peak intensity increases, and wavelength shifts from 440 nm to 433 nm, i.e., a blue shift occurs, designate AgNPs size decrease [20,76]. This may be because the faster consumption of reactant and the complete reduction of silver nitrate also occurs fast, causing faster color change [77].

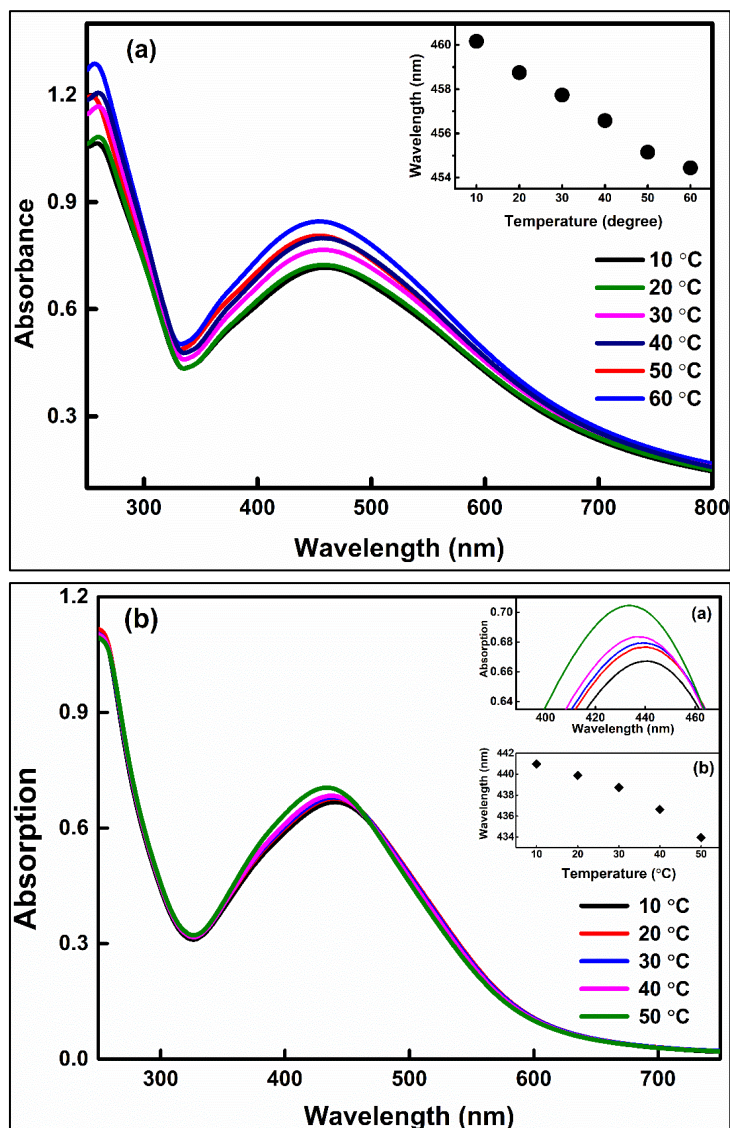


Figure 4.6. The absorption spectra of AgNPs in water at various temperatures using *Kalanchoe pinnata* (a) and *Abutilon theophrasti* (b) leaves. Inset shows the shift in band maximum as a function of temperature.

4.5 XRD PATTERN OF AgNPs

Fig. 14 illustrated the XRD pattern of AgNPs (AgNPs thin film coated on glass substrate) and indicated the crystalline structure. The estimated particle size using Scherer's relation corresponding to (111) peak is examined.

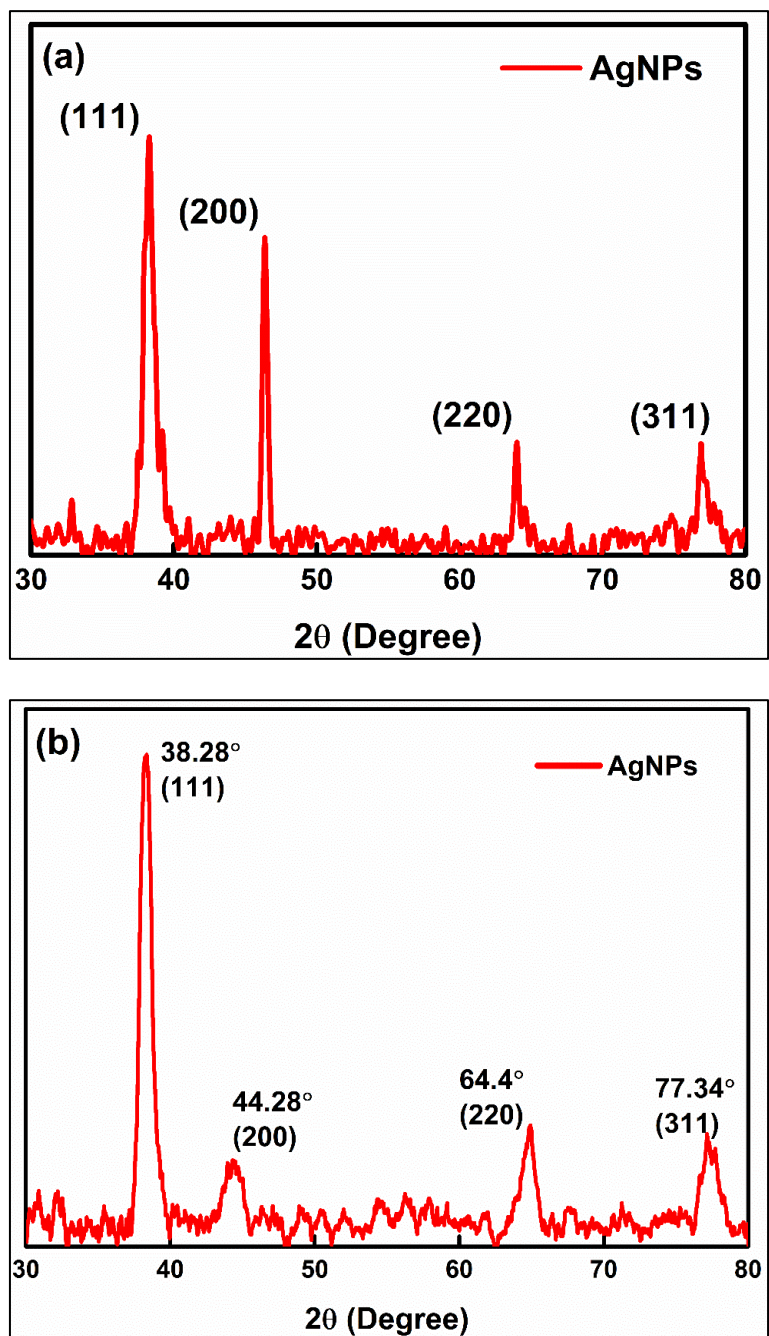


Figure 4.7. X-ray diffraction pattern of synthesized AgNPs using *Kalanchoe pinnata* (a) and *Abutilon theophrasti* (b) leaves.

4.5.1 Using *Kalanchoe pinnata*

There are four major reflection peaks at 2θ value of 38.26°, 44.47°, 64.71°, and 76.85°, which are index as (111), (200), (220), and (311) planes. (JCPDS, file No. 04-0783) [78,79]. The particle size estimated comes out to 36.9 nm.

4.5.2 Using *Abutilon theophrasti*

The XRD pattern of synthesized AgNPs and four major reflection peaks can be observed for (111), (200), (220), and (311) planes at 2θ equal to 38.28° , 44.28° , 64.4° , 77.34° respectively (JCPDS, file No. 04-0783) [80]. The particle size estimated comes out to 36.4 nm.

4.6 AgNPs MORPOLOGY

AgNPs shape and size were examined using FESEM and HRTEM. An aqueous solution of AgNPs was first allowed to settle on a quartz thin film and then FESEM images were taken, as shown in Fig. 4.8. For HRTEM images (Fig. 4.9), the AgNPs solution was sonicated and centrifuged, and AgNPs were coated on copper grid. A broad size distribution of nanoparticles was observed and agreed with the observed absorption and Zetasizer [81]. The shape of AgNPs observed from FESEM is spherical, which is in agreement with HRTEM results. Further, EDX analysis (Table 1) confirms the maximum presence of silver. In addition to Ag, Si, and O's existence is due to the use of the substrate, whereas Au is due to the gold coating over the thin film required for FESEM and EDX, as given in Fig. S1 of appendence.

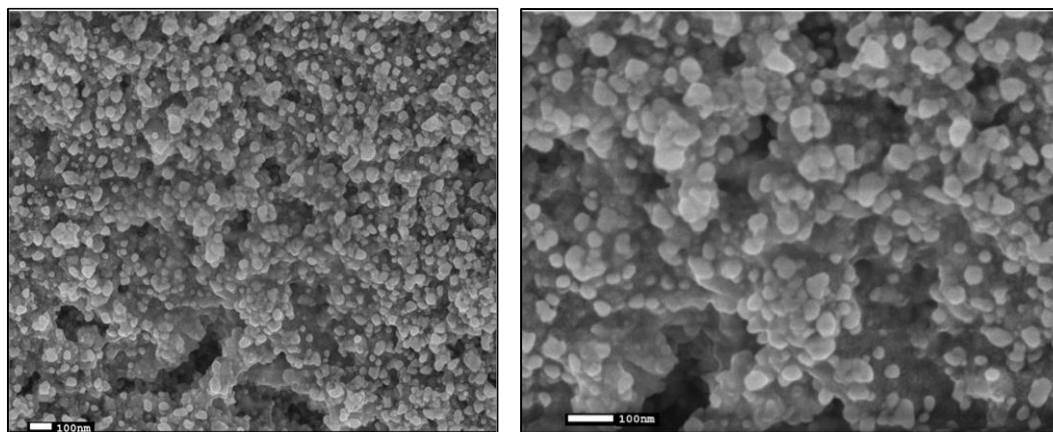


Figure 4.8 FESEM images of AgNPs thin film synthesized using *Kalanchoe pinnata* leaves.

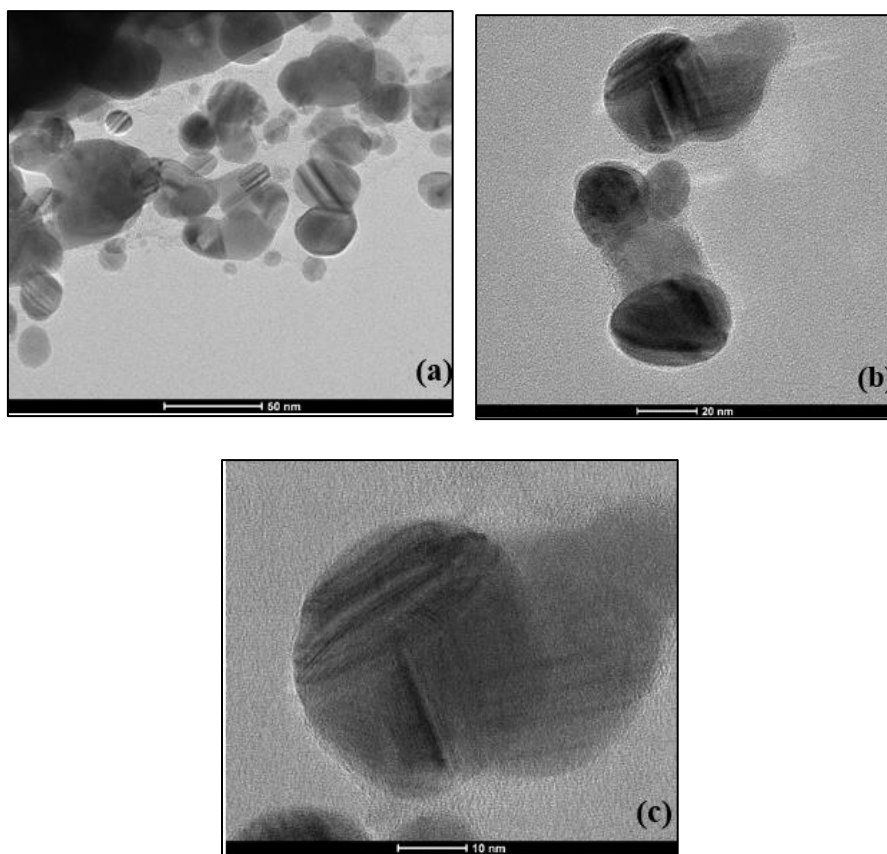


Figure 4.9. HRTEM images of AgNPs synthesized using *Kalanchoe pinnata* leaves extract at different magnifications.

Table 1: EDX analysis parameters of AgNPs recorded in thin-film.

Constituent	Weight %	Atomic %
C	4.93	21.65
O	11.1	36.58
Si	0.9	1.69
Au	2.37	0.63
Ag	80.7	39.45

4.7 ZETA POTENTIAL FOR SILVER NANOPARTICLES

4.7.1 Using *Kalanchoe pinnata*

Zeta potential affects the suspension stability and particle morphology [82]. It is the measurement of immensity and type of surface charges corresponding to double layer all over

the particles with high positive/negative values of zeta potential; accordingly, ± 30 mV is considered a more stable colloidal solution due to electrostatic attraction/repulsion among the particles [83]. It is related to particle size and environmental factors like pH, ionic strength, and the type of ions present in suspension [84]. Fig. 4.10 (a) illustrates the particle size distribution and the highest intensity appeared for 37.8 nm and 43.8 nm NPs. Thus, the average distribution of AgNPs in colloidal solution is about 40.8 nm and the value of zeta potential is -26.7 mV, denoting higher AgNPs stability and colloidal dispersion. The detail of zeta potential is shown in Fig. S2 of appendence.

4.7.2 Using *Abutilon theophrasti*

The magnitude of zeta potential is -27 mV making the colloidal solution highly stable. Calculated average AgNPs size from zeta potential is 36 nm, as shown in Fig. 4.10(b).

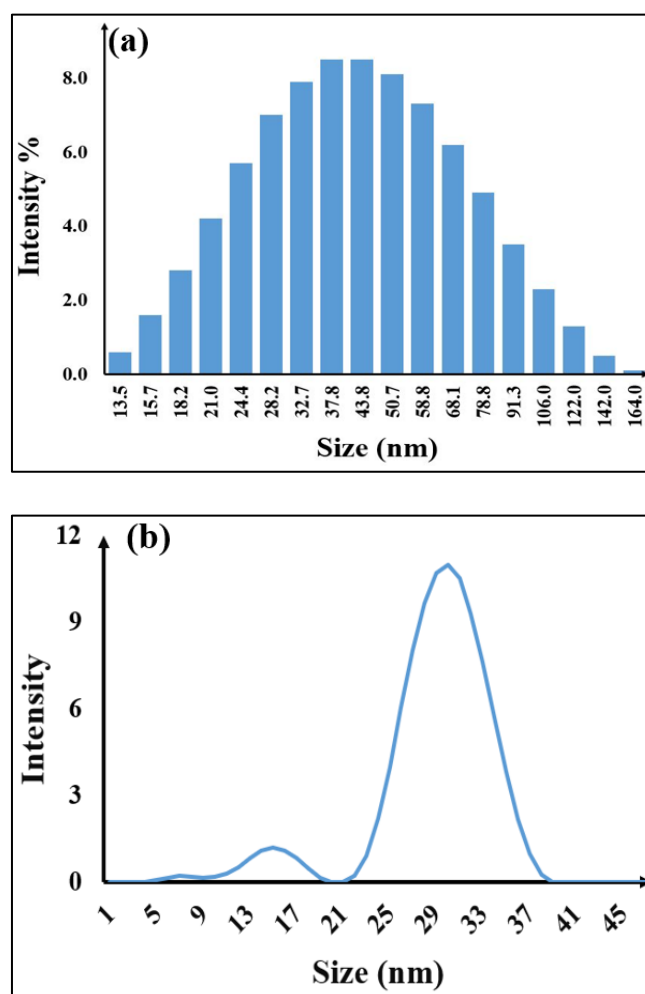


Figure 4.10. Particle size distribution for AgNPs synthesized using *Kalanchoe pinnata* (a) and *Abutilon theophrasti* (b) leaves extract.

4.8 AgNPs CATALYTIC ACTIVITY

AgNPs photocatalytic behaviour was examined with two hazardous dyes RhB and MO. For RhB the initial colour of dye-AgNPs solution was pink and for MO it was golden-orange. The initial absorption peak observed for RhB and MO were at 556 nm and 464 nm, respectively.

4.8.1 RhB degradation under UV irradiation

RhB was stored in dark and under UV lamp, the change in colour was observed from pink to colourless under UV irradiation as shown in Fig. 18. Change in colour from amber (bright luminescence) to nearly colourless (nearly zero luminescence) under UV irradiation (Fig. S3 of appendence). Fig. 19 and Fig. 20 show the absorption spectra of RhB dye in dark conditions and under UV irradiation with time. Absorption spectra of the dye shows sharp band at 556 nm corresponds to the $n-\pi$ transitions (C=N, C=O groups) [69]. In presence of AgNPs, the absorption intensity decreases. As time passes, the absorption intensity decreases monotonically and becomes minimal within the time of 150 min under dark conditions. Decrease in absorption intensity of dye under the dark conditions is illustrated in Fig. 19 and UV-irradiation in Fig. 20. Under UV irradiation, the absorption intensity decreases quite fast by the AgNPs and is reduced entirely in 45 min. Thus, in the dark, the dye degradation process was relatively slow and took more time than dye degradation under UV irradiation. More electrons are available to oxygen from AgNPs under UV irradiation, increasing the reaction process [85]. Apart from decreasing the absorption intensity of the lowest band in the dark and UV irradiation, intermediate absorption band that arises at around 400 nm is significantly affected. Under UV-irradiation, the 414 nm band is pronounced with the passes of time and shifts toward blue (from 434 nm to 414 nm), which is considered to be the SPR band of AgNPs catalysts [86,87], shown in Fig. S4 of appendence. Percentage of dye degradation calculated using $[(C_0-C_t)/C_0] \times 100$ is about 87 % and 83 % in the dark (150 min) and under UV-irradiation (45 min), respectively. The term C_t and C_0 represent concentration after time t and initial concentration.

The reaction rate constant k for dye degradation by AgNPs was estimated with $\ln(C/C_0) = -kt$ [87], as shown in Fig. 21, indicating that the dye degradation follows pseudo 1st order kinetics. The k value in the dark is 0.013 min^{-1} and under UV-irradiation is 0.042 min^{-1} . The photocatalytic reduction of dye was observed due to the excitation of SPR in AgNPs [88]. With UV-irradiation, the electron present in valence band will move from conduction band, making a hole (h^+_{VB}) at the lower band and electron (e^-_{CB}) in the upper band [89]. Excited electrons

available at AgNPs surfaces interact with oxygen molecules and produce super-oxygen ions ($\cdot\text{O}^{2-}$) and hydroxyl radicals ($\cdot\text{OH}$) [89]. The nanoparticles and radical ions react with dye and degrade it into smaller constituents and in CO_2 and H_2O [68,69,92–95].

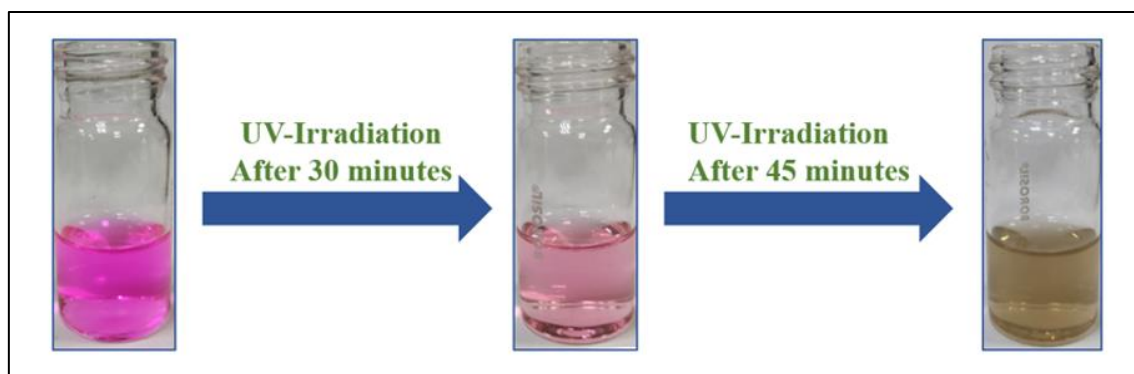


Figure 4.11. Change in colour of RhB dye ($10\ \mu\text{M}$) dissolved in water in the presence of AgNPs with doses of UV-light irradiations.

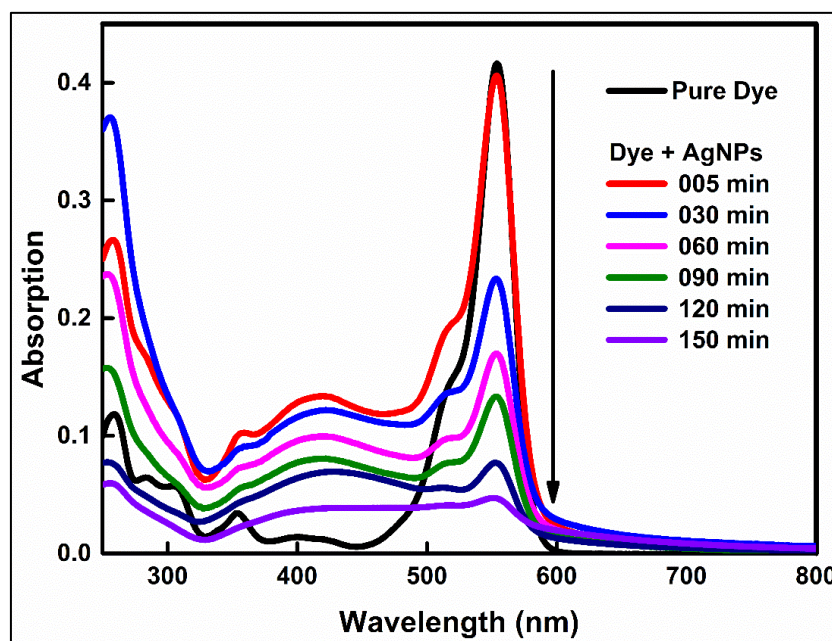


Figure 4.12. The absorption spectra of RhB dye in water in the presence of AgNPs at different time intervals in the dark.

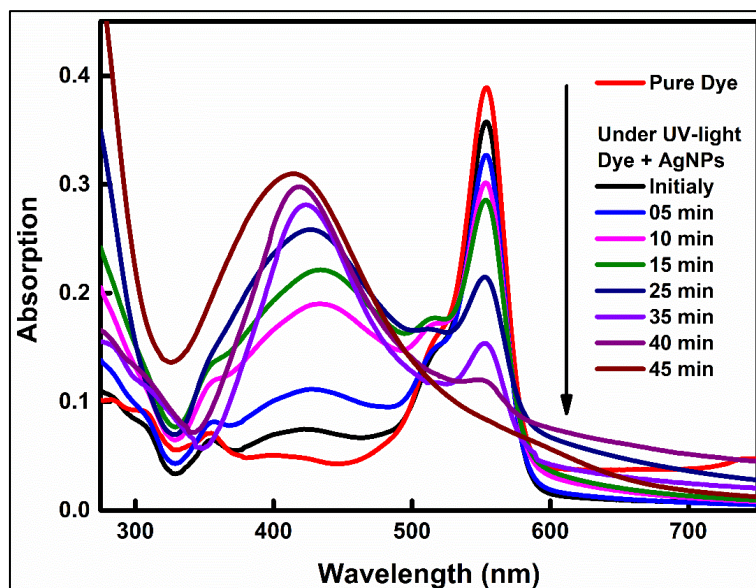


Figure 4.13. The absorption spectra of RhB dye in water in the presence of AgNPs at different time intervals under UV irradiation.

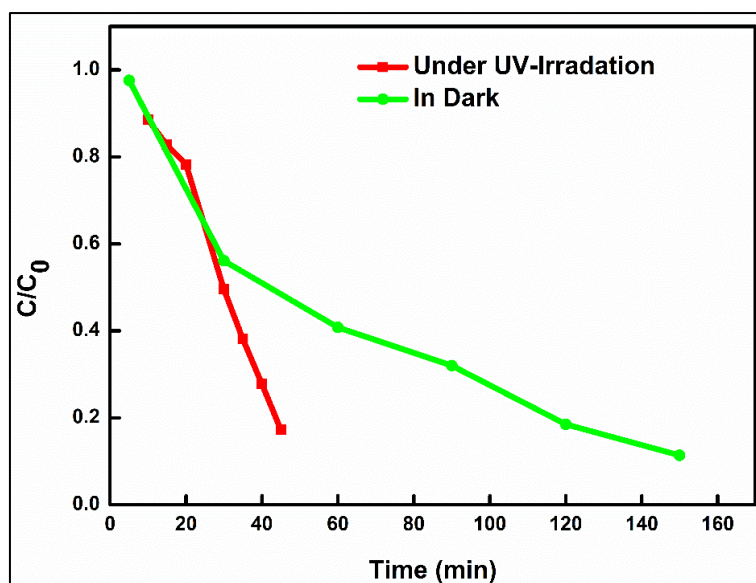


Figure 4.14. Plots of C/C_0 against reaction time for reducing RhB dye in the presence of AgNPs in the dark and under UV light.

4.8.2 MO degradation under Sunlight

The absorption maximum of MO is observed at 464 nm, and gradually decreasing when irradiated with sunlight. In dark, 25.4% of the dye is degraded in 35 min and whereas under

sunlight, nearly 74 % of the dye is degraded in the same reaction time and AgNPs concentration. The color change from orange to colourless under sunlight and light orange in dark shown in Fig.22. Absorption spectra of MO in dark and under sunlight are shown in Fig. 23 (a, b). The k value for dark is 0.0084/min, and under sunlight is 0.0366/min as shown in Fig 24. AgNPs photocatalytic activity in sunlight is due to excitation of SPR. The Ag conduction electron gets excited and captured by oxygen molecules which produce hydroxyl radicals and are responsible for MO dye degradation [94].

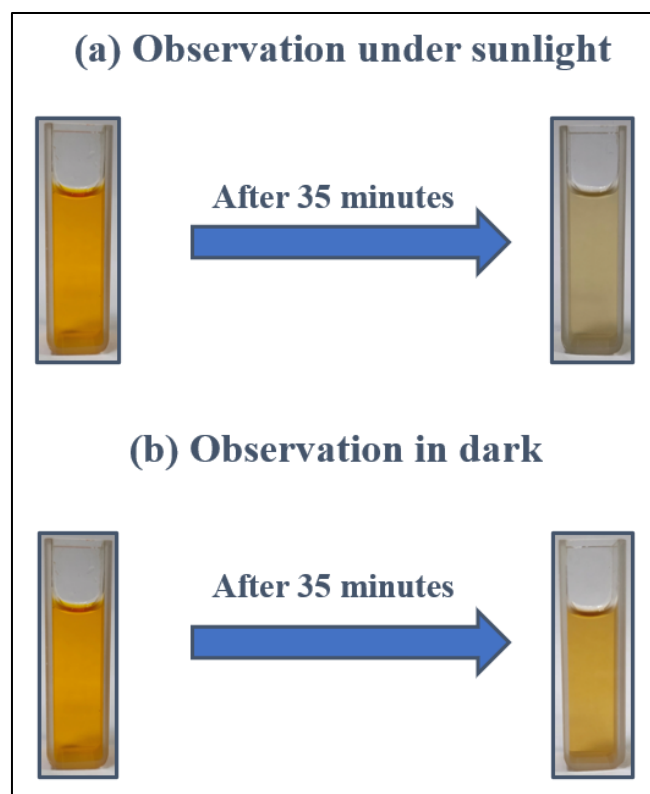


Figure 4.15. Change in color of the dye MO, after degradation under sunlight (a) and dark conditions (b).

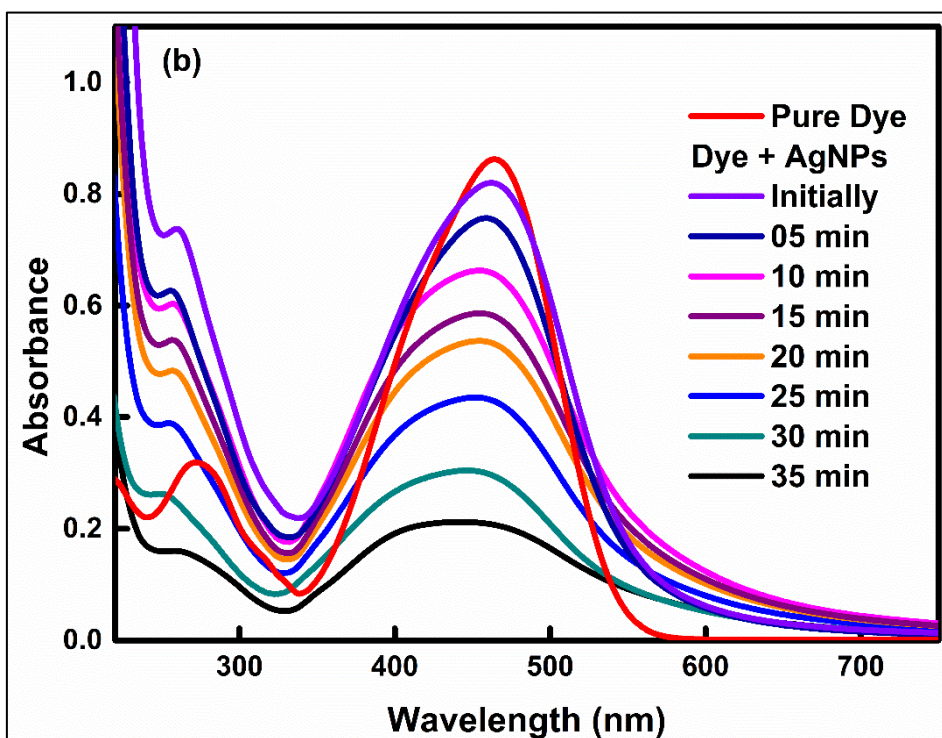
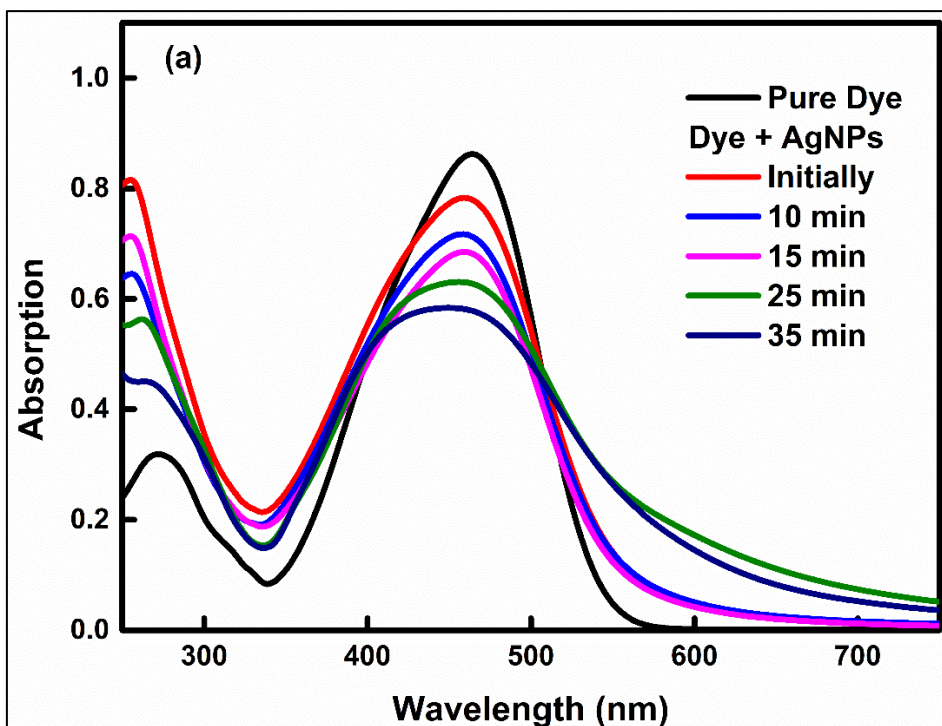


Figure 4.16. Absorption spectra of MO dye solution in water at different reaction times in the presence of AgNPs under dark conditions (a) and sunlight (b).

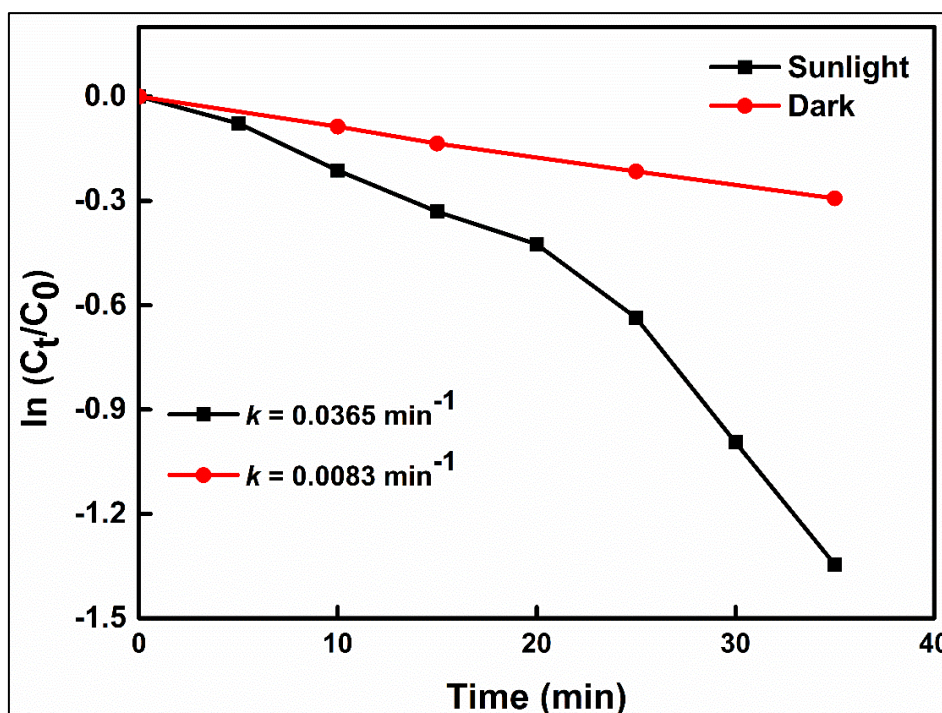


Figure 4.17. Plots of $\ln(C_t/C_0)$ against reaction time for reducing MO dye in the presence of AgNPs in the dark and under sunlight.

4.9 ANTIBACTERIAL ACTIVITY OF AgNPs

Bryophyllum pinnatum is known as an herbal plant with leaves having antibacterial properties [95,96]. Plant extract of *Bryophyllum pinnatum* contains photochemical such as flavonoids, polyphenols, terpenoids, alkaloids, and organic acids and are responsible for the biological activity of plant such as antimicrobial and antibacterial. They form complex free radical species with cell membranes affecting the overall functioning of bacterial cells [97,98]. AgNPs synthesized using *Bryophyllum pinnatum* leaves extract increases antibacterial properties; this is also due to their smaller size and reactivity. For antibacterial activity of AgNPs disk diffusion method was used against gram-negative bacteria [99]. Fig. 4.18 shows the antibacterial activities of AgNPs along with the leaves extract and silver salt. Antibacterial property of AgNPs are demonstrated by diameter of the zone of inhibition [51], proceeding 36 h in

incubation at 37 °C. The zone of inhibition for gram-negative (*E. coli*) is shown in Table 2. It can be seen that a higher zone of inhibition was observed for AgNPs against *E. coli* (gram-negative) bacteria compared to neat plant extract or silver nitrate. Water was taken as standard and silver salt was taken as control in antibacterial study. The AgNPs antibacterial activity is better than AgNO₃ and plant extract due to AgNPs smaller size. Smaller AgNPs can penetrate through a more extensive range of bacterial cells, causing a more extensive zone of inhibition of AgNPs. Note that the bacteria are cultured by giving appropriate conditions overnight and were diluted to 1.0×10^{-7} colony. Negative charges present on surface of cell membrane of bacteria and positive charges of Ag⁺, there is an electrostatic attraction between them, resulting in penetration of the cell membrane. When AgNPs penetrate the cell, they have the ability to alter physical and chemical properties by interacting with cellular structure and biomolecules of the cell, causing malfunctioning in normal physiological properties such as respiration and permeability of the cell. Further, AgNPs interact with biomolecules of cells forming various oxygen and nitro species that cause stress in the cell's DNA and leads to cell's death [49,50].

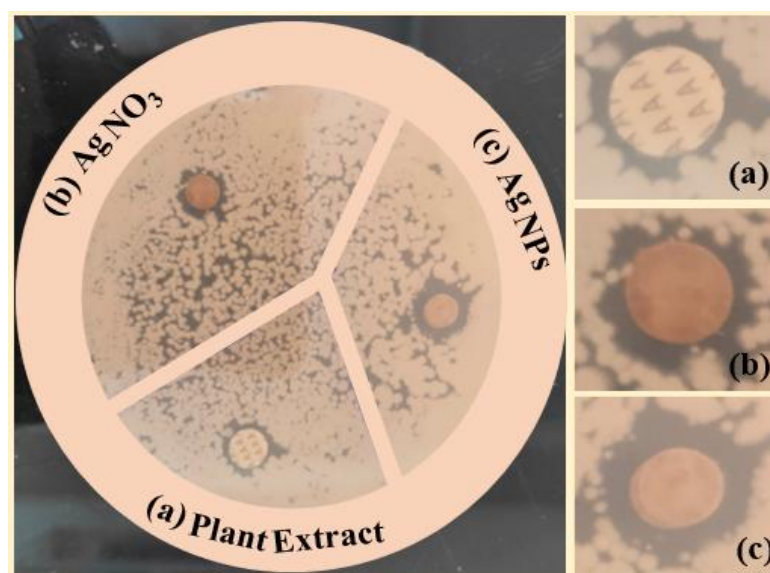


Figure 4.18 Zone of inhibition of *E-coli* bacteria treated with *Kalanchoe pinnata* leaves extract (a), silver nitrate (b), and AgNPs (c).

Table 2: Zone of inhibition for plant extract, AgNO₃ and AgNPs treated with *E. coli* bacterial strain.

S. No.	Sample Name	Zone of Inhibition (mm)
1	Plant Extract	7.88
2	AgNO ₃	8.80
3	AgNPs	11.90

CHAPTER 5

CONCLUSION

AgNPs were synthesized by an eco-friendly and convenient green process using the herbal plant *Kalanchoe pinnata* and *Abutilon theophrasti* leaves extracts. pH, temperature, concentrations and reaction time effect were studied, confirming the alkaline pH and high temperature were highly suitable for AgNPs synthesis. A strong SPR band occurs with a maximum between 420 nm to 440 nm. The XRD, TEM, and SEM results. XRD analysis indicates the crystalline nature of AgNPs, whereas the significant value of zeta potential has proven their high stability. The shape of AgNPs is nearly spherical. The comparison of photocatalyst degradation of RhB dye under UV-light and dark revealed that dye is degraded faster under UV-irradiation using *Kalanchoe pinnata* AgNPs. About 83 % dye was degraded in 45 min under UV-irradiation with a rate constant (k) of 0.042 min^{-1} and 87 % in the dark in 150 min with a k of 0.013 min^{-1} . The value of k is nearly three times higher for dye degradation under UV irradiation than dye degradation in the dark. The AgNPs (*Abutilon theophrasti*) are used to degrade MO dye. The k value for dark is $0.0084/\text{min}$, and under sunlight is $0.0366/\text{min}$, the reduction rate of dye is higher under sunlight using AgNPs (*Abutilon theophrasti*). The bio-synthesized AgNPs (*Kalanchoe pinnata*) reveal enhanced antibacterial activities against *E. coli* bacterial strains. Thus, dye degradation with eco-friendly AgNPs is highly beneficial for industrial applications and its antibacterial activities for medical applications.

APPENDICES

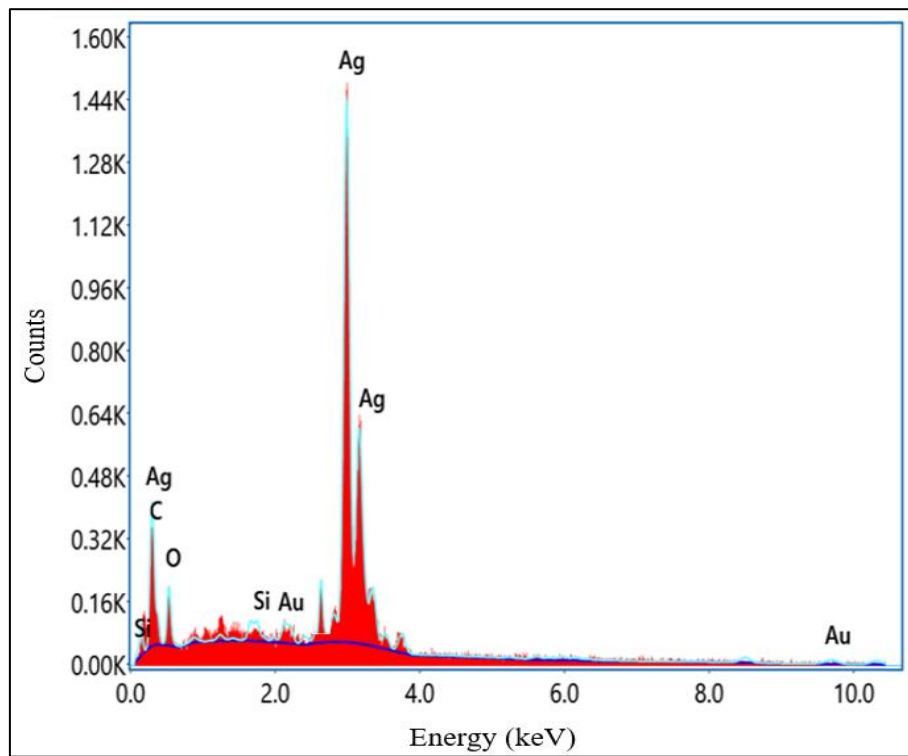


Figure S1.EDX spectrum of AgNPs, demonstrating the presence/formation AgNPs.

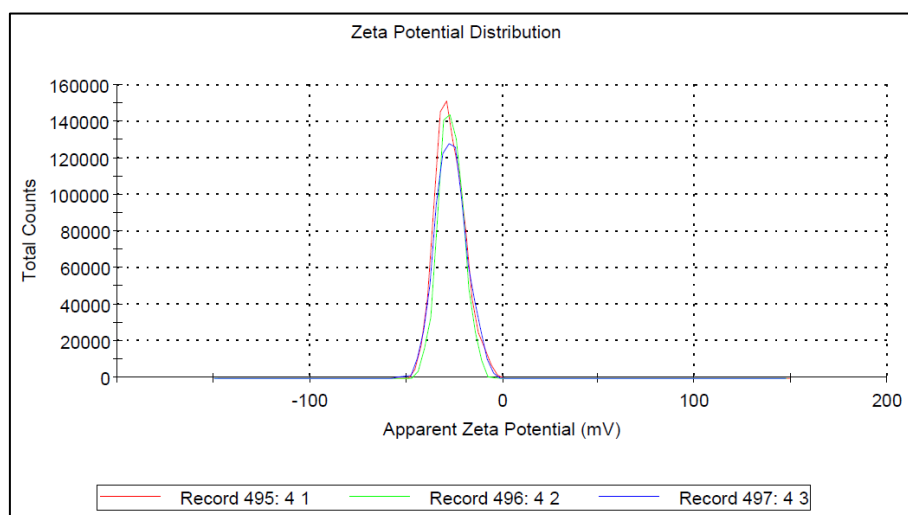


Figure S2. Zeta potential measurements of silver nanoparticles.

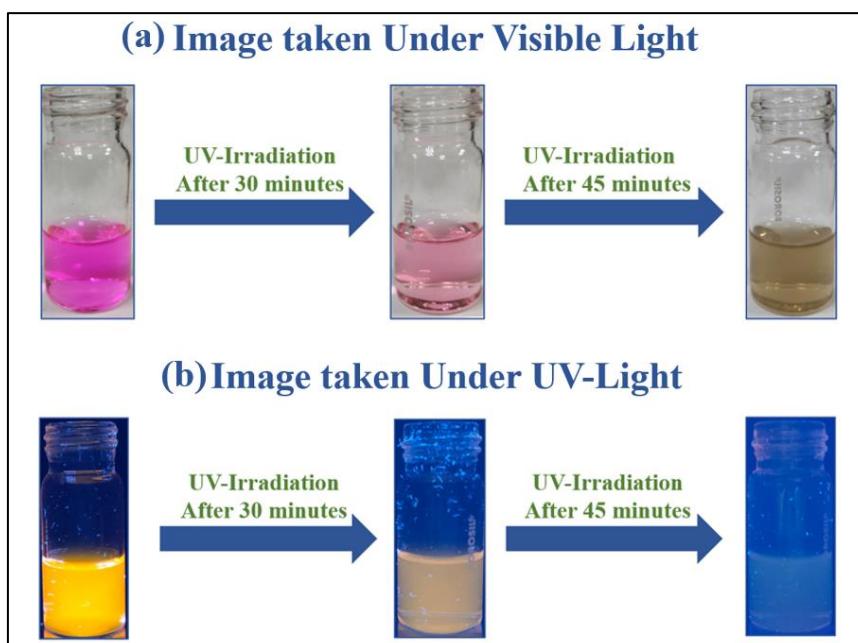


Figure S3. Change in colour of RhB dye ($10 \mu\text{M}$) dissolved in water in the presence of AgNPs with doses of UV-light irradiations taken in visible light (a). The colour of the dye solution changed from amber (bright luminescence) to nearly colourless (nearly zero luminescence) under UV irradiation (b).

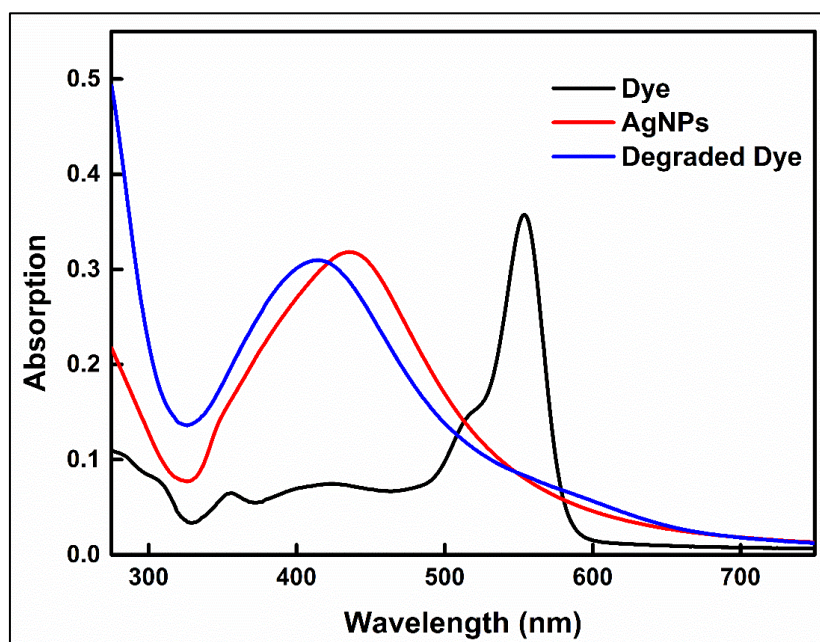


Figure S4. The absorption spectrum of initial dye, AgNPs, and final degraded dye under UV irradiation.

REFERENCES

- [1] J. E. Hulla, S. C. Sahu, and A. W. Hayes, "Nanotechnology: History and future," *Hum. Exp[1] J.E. Hulla, S.C. Sahu, A.W. Hayes, Nanotechnol. Hist. Futur. Hum. Exp. Toxicol.* 34 1318–1321. <https://doi.org/10.1177/0960327115603588>. *Experimental Toxicol.*, vol. 34, no. 12, pp. 1318–1321, 2015, doi: 10.1177/0960327115603588.
- [2] R. Baboo, "Ancient Indian Culture and Nanotechnology," *Int. J. Res. Anal. Rev.*, vol. 2, no. 3, pp. 97–99, 2015.
- [3] E. Angeli *et al.*, "Nanotechnology applications in medicine," *Tumori*, vol. 94, no. 2, pp. 206–215, 2008, doi: 10.1177/030089160809400213.
- [4] M. D. Cheng, "Effects of nanophase materials (≤ 20 nm) on biological responses," *J. Environ. Sci. Heal. - Part A Toxic/Hazardous Subst. Environ. Eng.*, vol. 39, no. 10, pp. 2691–2705, 2004, doi: 10.1081/ESE-200027028.
- [5] M. Mazur, "Electrochemically prepared silver nanoflakes and nanowires," *Electrochem. commun.*, vol. 6, no. 4, pp. 400–403, 2004, doi: 10.1016/j.elecom.2004.02.011.
- [6] S. H. Lee and B. H. Jun, "Silver nanoparticles: Synthesis and application for nanomedicine," *International Journal of Molecular Sciences*, vol. 20, no. 4, pp. 865–889, 2019, doi: 10.3390/ijms20040865.
- [7] X. Luo, A. Morrin, A. J. Killard, and M. R. Smyth, "Application of nanoparticles in electrochemical sensors and biosensors," *Electroanalysis*, vol. 18, no. 4, pp. 319–326, 2006, doi: 10.1002/elan.200503415.
- [8] P. N. Sudha, K. Sangeetha, K. Vijayalakshmi, and A. Barhoum, "Nanomaterials history, classification, unique properties, production and market," *Emerg. Appl. Nanoparticles Archit. Nanostructures Curr. Prospect. Futur. Trends*, vol. 12, pp. 341–384, 2018, doi: 10.1016/B978-0-323-51254-1.00012-9.
- [9] I. Khan, K. Saeed, and I. Khan, "Nanoparticles: Properties, applications and toxicities," *Arab. J. Chem.*, vol. 12, no. 7, pp. 908–931, 2019, doi: 10.1016/j.arabjc.2017.05.011.
- [10] P. I. Kattan, "Ratio of Surface Area to Volume in Nanotechnology and Nanoscience," *Basic Nanomechanics*, vol. i, no. January 2011, pp. 0–32, 2016.

- [11] L. Wei, J. Lu, H. Xu, A. Patel, Z. S. Chen, and G. Chen, "Silver nanoparticles: Synthesis, properties, and therapeutic applications," *Drug Discov. Today*, vol. 20, no. 5, pp. 595–601, 2015, doi: 10.1016/j.drudis.2014.11.014.
- [12] A. Verma and M. S. Mehata, "Controllable synthesis of silver nanoparticles using Neem leaves and their antimicrobial activity," *J. Radiat. Res. Appl. Sci.*, vol. 9, no. 1, pp. 109–115, 2016, doi: 10.1016/j.jrras.2015.11.001.
- [13] P. Mohanpuria, N. K. Rana, and S. K. Yadav, "Biosynthesis of nanoparticles: Technological concepts and future applications," *Journal of Nanoparticle Research*, vol. 10, no. 3. Springer, pp. 507–517, Mar. 2008, doi: 10.1007/s11051-007-9275-x.
- [14] A. V. Rane *et al.*, "Methods for Synthesis of Nanoparticles and Fabrication of Nanocomposites," *Chem. Rev.*, vol. 104, no. 9, pp. 3893–3946, 2004.
- [15] P. Iqbal, J. A. Preece, and P. M. Mendes, "Nanotechnology: The 'Top-Down' and 'Bottom-Up' Approaches," *Supramol. Chem.*, 2012, doi: 10.1002/9780470661345.smc195.
- [16] I. Ijaz, E. Gilani, A. Nazir, and A. Bukhari, "Detail review on chemical, physical and green synthesis, classification, characterizations and applications of nanoparticles," *Green Chem. Lett. Rev.*, vol. 13, no. 3, pp. 59–81, 2020, doi: 10.1080/17518253.2020.1802517.
- [17] N. Marquestaut, Y. Petit, A. Royon, P. Mounaix, T. Cardinal, and L. Canioni, "Three-Dimensional Silver Nanoparticle Formation Using Femtosecond Laser Irradiation in Phosphate Glasses: Analogy with Photography," *Adv. Funct. Mater.*, vol. 24, no. 37, pp. 5824–5832, Oct. 2014, doi: 10.1002/adfm.201401103.
- [18] M. Goudarzi, N. Mir, M. Mousavi-Kamazani, S. Bagheri, and M. Salavati-Niasari, "Biosynthesis and characterization of silver nanoparticles prepared from two novel natural precursors by facile thermal decomposition methods," *Sci. Rep.*, vol. 6, no. 1, pp. 1–13, Sep. 2016, doi: 10.1038/srep32539.
- [19] Y. C. Liu and L. H. Lin, "New pathway for the synthesis of ultrafine silver nanoparticles from bulk silver substrates in aqueous solutions by sonoelectrochemical methods," *Electrochem. commun.*, vol. 6, no. 11, pp. 1163–1168, Nov. 2004, doi: 10.1016/j.elecom.2004.09.010.

- [20] S. Jain and M. S. Mehata, "Medicinal Plant Leaf Extract and Pure Flavonoid Mediated Green Synthesis of Silver Nanoparticles and their Enhanced Antibacterial Property," *Sci. Rep.*, vol. 15867, no. January, pp. 1–13, 2017, doi: 10.1038/s41598-017-15724-8.
- [21] M. Sastry, A. Ahmad, M. I. Khan, and R. Kumar, "Microbial Nanoparticle Production," in *Nanobiotechnology*, Weinheim, FRG: Wiley-VCH Verlag GmbH & Co. KGaA, 2005, pp. 126–135.
- [22] P. Malik, R. Shankar, V. Malik, N. Sharma, and T. K. Mukherjee, "Green Chemistry Based Benign Routes for Nanoparticle Synthesis," *J. Nanoparticles*, vol. 2014, pp. 1–14, 2014, doi: 10.1155/2014/302429.
- [23] D. Bhattacharya and R. K. Gupta, "Nanotechnology and potential of microorganisms," *Critical Reviews in Biotechnology*, vol. 25, no. 4. Crit Rev Biotechnol, pp. 199–204, Dec. 2005, doi: 10.1080/07388550500361994.
- [24] D. Bose and S. Chatterjee, "Biogenic synthesis of silver nanoparticles using guava (*Psidium guajava*) leaf extract and its antibacterial activity against *Pseudomonas aeruginosa*," *Appl. Nanosci.*, vol. 6, no. 6, pp. 895–901, 2016, doi: 10.1007/s13204-015-0496-5.
- [25] M. Gericke and A. Pinches, "Biological synthesis of metal nanoparticles," *Hydrometallurgy*, vol. 83, no. 1–4, pp. 132–140, 2006, doi: 10.1016/j.hydromet.2006.03.019.
- [26] D. Mandal, M. E. Bolander, D. Mukhopadhyay, G. Sarkar, and P. Mukherjee, "The use of microorganisms for the formation of metal nanoparticles and their application," *Appl. Microbiol. Biotechnol.*, vol. 69, no. 5, pp. 485–492, 2006, doi: 10.1007/s00253-005-0179-3.
- [27] J. Xie, J. Y. Lee, D. I. C. Wang, and Y. P. Ting, "Silver nanoplates: From biological to biomimetic synthesis," *ACS Nano*, vol. 1, no. 5, pp. 429–439, Dec. 2007, doi: 10.1021/nm7000883.
- [28] Á. de Jesús Ruíz-Baltazar, S. Y. Reyes-López, D. Larrañaga, M. Estévez, and R. Pérez, "Green synthesis of silver nanoparticles using a *Melissa officinalis* leaf extract with antibacterial properties," *Results Phys.*, vol. 7, pp. 2639–2643, Jan. 2017, doi: 10.1016/j.rinp.2017.07.044.

- [29] G. Singhal, R. Bhavesh, K. Kasariya, A. R. Sharma, and R. P. Singh, "Biosynthesis of silver nanoparticles using *Ocimum sanctum* (Tulsi) leaf extract and screening its antimicrobial activity," *J. Nanoparticle Res.*, vol. 13, no. 7, pp. 2981–2988, Jul. 2011, doi: 10.1007/s11051-010-0193-y.
- [30] Z. Xu and M. Deng, "Identification and Control of Common Weeds: Volume 2," *Identif. Control Common Weeds Vol. 2*, vol. 2, pp. 475–486, 2017, doi: 10.1007/978-94-024-1157-7.
- [31] R. Gupta, M. Lohani, and S. Arora, "ANTI-INFLAMMATORY ACTIVITY OF THE LEAF EXTRACTS / FRACTIONS OF BRYOPHYLLUM PINNATUM SALIV . SYN," vol. 3, no. 1, pp. 16–18, 2010.
- [32] J. A. O. Ojewole, "Antinociceptive , anti-inflammatory and antidiabetic effects of *Bryophyllum pinnatum* (Crassulaceae) leaf aqueous extract," vol. 99, pp. 13–19, 2005, doi: 10.1016/j.jep.2005.01.025.
- [33] M. Yadav, V. Gulkari, and M. Wanjari, "Bryophyllum pinnatum leaf extracts prevent formation of renal calculi in lithiatic rats," *Anc. Sci. Life*, vol. 36, no. 2, pp. 90–100, 2016, doi: 10.4103/asl.asl_90_16.
- [34] A. Sohgaura, P. Bigoniya, and B. Shrivastava, "In vitro antilithiatic potential of *Kalanchoe pinnata*, *Embllica officinalis*, *Bambusa nutans*, and *Cynodon dactylon*," *J. Pharm. Bioallied Sci.*, vol. 10, no. 2, pp. 83–89, 2018, doi: 10.4103/JPBS.JPBS_18_18.
- [35] M. Rafique, I. Sadaf, M. S. Rafique, and M. B. Tahir, "A review on green synthesis of silver nanoparticles and their applications," *Artif. Cells, Nanomedicine Biotechnol.*, vol. 45, no. 7, pp. 1272–1291, 2017, doi: 10.1080/21691401.2016.1241792.
- [36] M. F. Lengke, M. E. Fleet, and G. Southam, "Biosynthesis of silver nanoparticles by filamentous cyanobacteria from a silver(I) nitrate complex," *Langmuir*, vol. 23, no. 5, pp. 2694–2699, 2007, doi: 10.1021/la0613124.
- [37] H. Jiale *et al.*, "Biosynthesis of silver and gold nanoparticles by novel sundried *Cinnamomum camphora* leaf," *Nanotechnology*, vol. 18, no. 10, pp. 105104–105116, 2007, [Online]. Available: <http://stacks.iop.org/0957-4484/18/i=10/a=105104>.
- [38] D. Raju, U. J. Mehta, and S. Hazra, "Synthesis of gold nanotriangles and silver nanoparticles using *Aloe vera* plant extract.," *Trees (Berl. West)*, vol. 25, no. 2, pp. 577–

- 583, 2011, doi: 10.1021/nl015673+.
- [39] S. Li *et al.*, “Green synthesis of silver nanoparticles using *Capsicum annum* L. Extract,” *Green Chem.*, vol. 9, no. 8, pp. 852–85, 2007, doi: 10.1039/b615357g.
- [40] J. L. Gardea-Torresdey, E. Gomez, J. R. Peralta-Videa, J. G. Parsons, H. Troiani, and M. Jose-Yacaman, “Alfalfa sprouts: A natural source for the synthesis of silver nanoparticles,” *Langmuir*, vol. 19, no. 4, pp. 1357–1361, 2003, doi: 10.1021/la020835i.
- [41] Hutchison JE., “Greener nanoscience: a proactive approach to advancing applications and reducing implications of nanotechnology.,” *ACS Nano*, vol. 2, pp. 395–402, 2008, doi: <https://doi.org/10.1021/nm800131j>.
- [42] I. Hussain, M. Brust, A. J. Papworth, and A. I. Cooper, “Preparation of acrylate-stabilized gold and silver hydrosols and gold-polymer composite films,” *Langmuir*, vol. 19, no. 11, pp. 4831–4835, 2003, doi: 10.1021/la020710d.
- [43] V. K. Sharma, R. A. Yngard, and Y. Lin, “Silver nanoparticles: Green synthesis and their antimicrobial activities,” *Adv. Colloid Interface Sci.*, vol. 145, no. 1–2, pp. 83–96, 2009, doi: 10.1016/j.cis.2008.09.002.
- [44] M. A. Albrecht, C. W. Evans, and C. L. Raston, “Green chemistry and the health implications of nanoparticles,” *Green Chem.*, vol. 8, no. 5, pp. 417–432, 2006, doi: 10.1039/b517131h.
- [45] J. Brown, “Impact of silver nanoparticles on wastewater treatment,” *Nanotechnologies Environ. Remediat. Appl. Implic.*, pp. 255–267, 2017, doi: 10.1007/978-3-319-53162-5_9.
- [46] N. Z. Mamadalieva, F. Sharopov, J. P. Giraultc, M. Wink, and R. Lafont, “Phytochemical analysis and bioactivity of the aerial parts of *Abutilon theophrasti* (Malvaceae), a medicinal weed,” *Nat. Prod. Res.*, vol. 28, no. 20, pp. 1777–1779, 2014, doi: 10.1080/14786419.2014.939080.
- [47] M. Dinu *et al.*, “Proximate composition and some physico-chemical properties of *abutilon theophrasti* (velvetleaf) seed oil,” *Rev. Chim.*, vol. 61, no. 1, pp. 50–54, 2010.
- [48] S. Unser, I. Bruzas, J. He, and L. Sagle, “Localized Surface Plasmon Resonance Biosensing: Current Challenges and Approaches,” *Sensors*, vol. 15, no. 7, pp. 15684–15716, Jul. 2015, doi: 10.3390/s150715684.

- [49] Y. Qing *et al.*, “Potential antibacterial mechanism of silver nanoparticles and the optimization of orthopedic implants by advanced modification technologies,” *Int. J. Nanomedicine*, vol. 13, pp. 3311–3327, 2018, doi: 10.2147/IJN.S165125.
- [50] P. V. AshaRani, G. L. K. Mun, M. P. Hande, and S. Valiyaveetil, “Cytotoxicity and genotoxicity of silver nanoparticles in human cells,” *ACS Nano*, vol. 3, no. 2, pp. 279–290, 2009, doi: 10.1021/nn800596w.
- [51] J. K. Patra and K. H. Baek, “Antibacterial activity and synergistic antibacterial potential of biosynthesized silver nanoparticles against foodborne pathogenic bacteria along with its anticandidal and antioxidant effects,” *Front. Microbiol.*, vol. 8, no. FEB, pp. 167–181, Feb. 2017, doi: 10.3389/fmicb.2017.00167.
- [52] S. V. Kulkarni, C. D. Blackwell, A. L. Blackard, C. W. Stackhouse, and M. W. Alexander, “Textile dyes and dyeing equipment: classification, properties, and environmental aspects,” *Environ. Prot. Agency*, vol. 85, pp. 600–603, 1985.
- [53] K. -T Chung and S. E. Stevens, “Degradation azo dyes by environmental microorganisms and helminths,” *Environ. Toxicol. Chem.*, vol. 12, no. 11, pp. 2121–2132, 1993, doi: 10.1002/etc.5620121120.
- [54] H. Kolya, P. Maiti, A. Pandey, and T. Tripathy, “Green synthesis of silver nanoparticles with antimicrobial and azo dye (Congo red) degradation properties using *Amaranthus gangeticus* Linn leaf extract,” *J. Anal. Sci. Technol.*, vol. 6, no. 1, p. 33, Dec. 2015, doi: 10.1186/s40543-015-0074-1.
- [55] M. Ismail, M. I. Khan, M. A. Khan, K. Akhtar, A. M. Asiri, and S. B. Khan, “Plant-supported silver nanoparticles: Efficient, economically viable and easily recoverable catalyst for the reduction of organic pollutants,” *Appl. Organomet. Chem.*, vol. 33, no. 8, Aug. 2019, doi: 10.1002/aoc.4971.
- [56] B. Pant, P. S. Saud, M. Park, S. J. Park, and H. Y. Kim, “General one-pot strategy to prepare Ag–TiO₂ decorated reduced graphene oxide nanocomposites for chemical and biological disinfectant,” *J. Alloys Compd.*, vol. 671, pp. 51–59, 2016, doi: 10.1016/j.jallcom.2016.02.067.
- [57] S. F. Kang, C. H. Liao, and S. T. Po, “Decolorization of textile wastewater by photo-fenton oxidation technology,” *Chemosphere*, vol. 41, no. 8, pp. 1287–1294, 2000, doi: 10.1016/S0045-6535(99)00524-X.

- [58] M. K. Singh and M. S. Mehata, "Phase-dependent optical and photocatalytic performance of synthesized titanium dioxide (TiO₂) nanoparticles," *Optik (Stuttg.)*, vol. 193, 2019, doi: 10.1016/j.ijleo.2019.163011.
- [59] P. Kumar, M. Govindaraju, S. Senthamilselvi, and K. Premkumar, "Photocatalytic degradation of methyl orange dye using silver (Ag) nanoparticles synthesized from *Ulva lactuca*," *Colloids Surfaces B Biointerfaces*, vol. 103, pp. 658–661, 2013, doi: 10.1016/j.colsurfb.2012.11.022.
- [60] Y. Xu, B. Ren, R. Wang, L. Zhang, T. Jiao, and Z. Liu, "Facile preparation of rod-like MnO nanomixtures via hydrothermal approach and highly efficient removal of methylene blue for wastewater treatment," *Nanomaterials*, vol. 9, no. 1, pp. 1–16, Jan. 2019, doi: <https://doi.org/10.3390/nano9010010>.
- [61] M. K. Singh and M. S. Mehata, "Enhanced photoinduced catalytic activity of transition metal ions incorporated TiO₂ nanoparticles for degradation of organic dye: Absorption and photoluminescence spectroscopy," *Opt. Mater. (Amst.)*, vol. 109, Nov. 2020, doi: 10.1016/j.optmat.2020.110309.
- [62] S. M. Albukhari, M. Ismail, K. Akhtar, and E. Y. Danish, "Catalytic reduction of nitrophenols and dyes using silver nanoparticles @ cellulose polymer paper for the resolution of waste water treatment challenges," *Colloids Surfaces A Physicochem. Eng. Asp.*, vol. 577, pp. 548–561, 2019, doi: 10.1016/j.colsurfa.2019.05.058.
- [63] K. Balan *et al.*, "Antidiabetic activity of silver nanoparticles from green synthesis using *Lonicera japonica* leaf extract," *RSC Adv.*, vol. 6, no. 46, pp. 40162–40168, Apr. 2016, doi: 10.1039/c5ra24391b.
- [64] C. Krishnaraj, E. G. Jagan, S. Rajasekar, P. Selvakumar, P. T. Kalaichelvan, and N. Mohan, "Synthesis of silver nanoparticles using *Acalypha indica* leaf extracts and its antibacterial activity against water borne pathogens," *Colloids Surfaces B Biointerfaces*, vol. 76, no. 1, pp. 50–56, 2010, doi: 10.1016/j.colsurfb.2009.10.008.
- [65] P. S. Sadalage, R. V. Patil, M. N. Padv, and K. D. Pawar, "Almond skin extract mediated optimally biosynthesized antibacterial silver nanoparticles enable selective and sensitive colorimetric detection of Fe⁺² ions," *Colloids Surfaces B Biointerfaces*, vol. 193, no. 0927–7765, pp. 1–11, 2020, doi: 10.1016/j.colsurfb.2020.111084.
- [66] S. Elzey and V. H. Grassian, "Agglomeration, isolation and dissolution of commercially

- manufactured silver nanoparticles in aqueous environments,” *J. Nanoparticle Res.*, vol. 12, no. 5, pp. 1945–1958, Jun. 2010, doi: 10.1007/s11051-009-9783-y.
- [67] M. K. Alqadi, O. A. Abo Noqtah, F. Y. Alzoubi, J. Alzouby, and K. Aljarrah, “PH effect on the aggregation of silver nanoparticles synthesized by chemical reduction,” *Mater. Sci. Pol.*, vol. 32, no. 1, pp. 107–111, Jan. 2014, doi: 10.2478/s13536-013-0166-9.
- [68] H. Zhang, B. Chen, and J. F. Banfield, “Particle size and pH effects on nanoparticle dissolution,” *J. Phys. Chem. C*, vol. 114, no. 35, pp. 14876–14884, Sep. 2010, doi: 10.1021/jp1060842.
- [69] N. T. K. Thanh, N. Maclean, and S. Mahiddine, “Mechanisms of nucleation and growth of nanoparticles in solution,” *Chemical Reviews*, vol. 114, no. 15. American Chemical Society, pp. 7610–7630, Aug. 2014, doi: 10.1021/cr400544s.
- [70] I. Fernando and Y. Zhou, “Impact of pH on the stability, dissolution and aggregation kinetics of silver nanoparticles,” *Chemosphere*, vol. 216, pp. 297–305, Feb. 2019, doi: 10.1016/j.chemosphere.2018.10.122.
- [71] H. M. M. Ibrahim, “Green synthesis and characterization of silver nanoparticles using banana peel extract and their antimicrobial activity against representative microorganisms,” *J. Radiat. Res. Appl. Sci.*, vol. 8, no. 3, pp. 265–275, 2015, doi: 10.1016/j.jrras.2015.01.007.
- [72] R. Veerasamy *et al.*, “Biosynthesis of silver nanoparticles using mangosteen leaf extract and evaluation of their antimicrobial activities,” *J. Saudi Chem. Soc.*, vol. 15, no. 2, pp. 113–120, 2011, doi: 10.1016/j.jscs.2010.06.004.
- [73] S. M. Roopan *et al.*, “Low-cost and eco-friendly phyto-synthesis of silver nanoparticles using *Cocos nucifera* coir extract and its larvicidal activity,” *Ind. Crops Prod.*, vol. 43, no. 1, pp. 631–635, 2013, doi: 10.1016/j.indcrop.2012.08.013.
- [74] X. C. Jiang, W. M. Chen, C. Y. Chen, S. X. Xiong, and A. B. Yu, “Role of Temperature in the Growth of Silver Nanoparticles Through a Synergetic Reduction Approach,” *Nanoscale Res. Lett.*, vol. 6, no. 1, pp. 1–9, 2011, doi: 10.1007/s11671-010-9780-1.
- [75] E. A. Terenteva, V. V. Apyari, S. G. Dmitrienko, and Y. A. Zolotov, “Formation of plasmonic silver nanoparticles by flavonoid reduction: A comparative study and application for determination of these substances,” *Spectrochim. Acta - Part A Mol.*

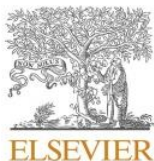
- Biomol. Spectrosc.*, vol. 151, pp. 89–95, Jun. 2015, doi: 10.1016/j.saa.2015.06.049.
- [76] K. Saware and A. Venkataraman, “Biosynthesis and Characterization of Stable Silver Nanoparticles Using *Ficus religiosa* Leaf Extract: A Mechanism Perspective,” *J. Clust. Sci.*, vol. 25, no. 4, pp. 1157–1171, 2014, doi: 10.1007/s10876-014-0697-1.
- [77] J. Park, J. Joo, S. G. Kwon, Y. Jang, and T. Hyeon, “Synthesis of Monodisperse Spherical Nanocrystals,” *ChemInform*, vol. 38, no. 33, p. (1-27), 2007, doi: 10.1002/chin.200733240.
- [78] Y. Meng, “A sustainable approach to fabricating ag nanoparticles/PVA hybrid nanofiber and its catalytic activity,” *Nanomaterials*, vol. 5, no. 2, pp. 1124–1135, 2015, doi: 10.3390/nano5021124.
- [79] R. I. Priyadarshini, G. Prasannaraj, N. Geetha, and P. Venkatachalam, “Microwave-Mediated Extracellular Synthesis of Metallic Silver and Zinc Oxide Nanoparticles Using Macro-Algae (*Gracilaria edulis*) Extracts and Its Anticancer Activity Against Human PC3 Cell Lines,” *Appl. Biochem. Biotechnol.*, vol. 174, no. 8, pp. 2777–2790, Nov. 2014, doi: 10.1007/s12010-014-1225-3.
- [80] R. Singh, S. K. Sahu, and M. Thangaraj, “Biosynthesis of Silver Nanoparticles by Marine Invertebrate (Polychaete) and Assessment of Its Efficacy against Human Pathogens,” *J. Nanoparticles*, vol. 2014, pp. 1–7, 2014, doi: 10.1155/2014/718240.
- [81] N. S. Pesika, K. J. Stebe, and P. C. Searson, “Relationship between Absorbance Spectra and Particle Size Distributions for Quantum-Sized Nanocrystals,” *J. Phys. Chem. B*, vol. 107, no. 38, pp. 10412–10415, Sep. 2003, doi: 10.1021/jp0303218.
- [82] A. Sankhla, R. Sharma, R. S. Yadav, D. Kashyap, S. L. Kothari, and S. Kachhwaha, “Biosynthesis and characterization of cadmium sulfide nanoparticles - An emphasis of zeta potential behavior due to capping,” *Mater. Chem. Phys.*, vol. 170, pp. 44–51, Feb. 2016, doi: 10.1016/j.matchemphys.2015.12.017.
- [83] R. Xu, “Progress in nanoparticles characterization: Sizing and zeta potential measurement,” *Particuology*, vol. 6, no. 2, pp. 112–115, 2008, doi: 10.1016/j.partic.2007.12.002.
- [84] A. M. El Badawy, T. P. Luxton, R. G. Silva, K. G. Scheckel, M. T. Suidan, and T. M. Tolaymat, “Impact of environmental conditions (pH, ionic strength, and electrolyte type)

- on the surface charge and aggregation of silver nanoparticles suspensions,” *Environ. Sci. Technol.*, vol. 44, no. 4, pp. 1260–1266, 2010, doi: 10.1021/es902240k.
- [85] X. Chen *et al.*, “Supported silver nanoparticles as photocatalysts under ultraviolet and visible light irradiation,” *pubs.rsc.org*, 2010, doi: 10.1039/b921696k.
- [86] S. Joseph and B. Mathew, “Facile synthesis of silver nanoparticles and their application in dye degradation,” *Mater. Sci. Eng. B Solid-State Mater. Adv. Technol.*, vol. 195, pp. 90–97, 2015, doi: 10.1016/j.mseb.2015.02.007.
- [87] M. Sundararajan, V. Sailaja, L. John Kennedy, and J. Judith Vijaya, “Photocatalytic degradation of rhodamine B under visible light using nanostructured zinc doped cobalt ferrite: Kinetics and mechanism,” *Ceram. Int.*, vol. 43, no. 1, pp. 540–548, 2017, doi: 10.1016/j.ceramint.2016.09.191.
- [88] M.A. Garcia, “Surface plasmons in metallic nanoparticles: fundamentals and applications,” *J. Phys. D. Appl. Phys.*, vol. 45, no. 38, p. 389501, 2012, doi: 10.1088/0022-3727/44/28/283001.
- [89] W. A. Shaikh, S. Chakraborty, and R. Ul Islam, “UV-assisted photo-catalytic degradation of anionic dye (Congo red) using biosynthesized silver nanoparticles: A green catalysis,” *Desalin. Water Treat.*, vol. 130, pp. 232–242, 2018, doi: 10.5004/dwt.2018.23004.
- [90] P. Khare *et al.*, “Sunlight-Induced Selective Photocatalytic Degradation of Methylene Blue in Bacterial Culture by Pollutant Soot Derived Nontoxic Graphene Nanosheets,” 2017, doi: 10.1021/acssuschemeng.7b02929.
- [91] Z. C. Wu, Y. Zhang, T. X. Tao, L. Zhang, and H. Fong, “Silver nanoparticles on amidoxime fibers for photo-catalytic degradation of organic dyes in waste water,” *Appl. Surf. Sci.*, vol. 257, no. 3, pp. 1092–1097, 2010, doi: 10.1016/j.apsusc.2010.08.022.
- [92] M. A. Mahmoud, A. Poncheri, Y. Badr, and M. G. Abd El Waned, “Photocatalytic degradation of methyl red dye,” *S. Afr. J. Sci.*, vol. 105, no. 7–8, pp. 299–303, Jul. 2009, doi: 10.4102/sajs.v105i7/8.86.
- [93] R. Karthik *et al.*, “Biosynthesis of silver nanoparticles by using *Camellia japonica* leaf extract for the electrocatalytic reduction of nitrobenzene and photocatalytic degradation of Eosin-Y,” *J. Photochem. Photobiol. B Biol.*, vol. 170, pp. 164–172, May 2017, doi:

10.1016/j.jphotobiol.2017.03.018.

- [94] L. Wang, F. Lu, Y. Liu, Y. Wu, and Z. Wu, “Photocatalytic degradation of organic dyes and antimicrobial activity of silver nanoparticles fast synthesized by flavonoids fraction of *Psidium guajava* L. leaves,” *J. Mol. Liq.*, vol. 263, pp. 187–192, Aug. 2018, doi: 10.1016/j.molliq.2018.04.151.
- [95] D. A. Akinpelu, “Antimicrobial activity of *Bryophyllum pinnatum* leaves,” *Fitoterapia*, vol. 71, no. 2, pp. 193–194, Apr. 2000, doi: 10.1016/S0367-326X(99)00135-5.
- [96] C. Liao, Y. Li, and S. C. Tjong, “Bactericidal and Cytotoxic Properties of Silver Nanoparticles,” *International Journal of Molecular Sciences*, vol. 20, no. 2. 2019, doi: 10.3390/ijms20020449.
- [97] B. Pant, M. Park, G. P. Ojha, D. U. Kim, H. Y. Kim, and S. J. Park, “Electrospun salicylic acid/polyurethane composite nanofibers for biomedical applications,” *Int. J. Polym. Mater. Polym. Biomater.*, vol. 67, no. 12, pp. 739–744, 2018, doi: 10.1080/00914037.2017.1376200.
- [98] A. Hassan, H. Ullah, and M. G. Bonomo, “Antibacterial and Antifungal Activities of the Medicinal Plant *Veronica biloba*,” *J. Chem.*, vol. 2019, 2019, doi: 10.1155/2019/5264943.
- [99] A. Klančnik, S. Piskernik, B. Jeršek, and S. S. Možina, “Evaluation of diffusion and dilution methods to determine the antibacterial activity of plant extracts,” *J. Microbiol. Methods*, vol. 81, no. 2, pp. 121–126, May 2010, doi: 10.1016/j.mimet.2010.02.004.

RESEARCH PAPER



Contents lists available at ScienceDirect

Chemical Physics Letters

journal homepage: www.elsevier.com/locate/cplett

Research paper

Green synthesis of silver nanoparticles using *Kalanchoe pinnata* leaves (life plant) and their antibacterial and photocatalytic activities

Aryan¹, Ruby¹, Mohan Singh Mehata^{*}

Laser-Spectroscopy Laboratory, Department of Applied Physics, Delhi Technological University, Bawana Road, Delhi 110042, India



ARTICLE INFO

Keywords:

Silver nanoparticles
Kalanchoe pinnata
 Antibacterial activities
 Photocatalysts
 Surface plasmon resonance

ABSTRACT

Silver nanoparticles (AgNPs) were synthesized via green synthesis using a new herbal plant *Kalanchoe pinnata* (known as life plant) leaves. Effects of physicochemical parameters like temperature, pH and concentration on AgNPs were examined, and the absorption spectra were observed due to strong surface plasmon resonance. The crystalline nature and stability of AgNPs were confirmed by XRD pattern and zeta potential, respectively. The morphology of AgNPs was studied using FESEM and HRTEM. AgNPs showed antibacterial activity against the gram-negative *E. Coli* bacteria and photocatalytic activity in the degradation of rhodamine B dye with a reaction rate constant of 0.042 min⁻¹.

1. Introduction

Nowadays, nanotechnology plays a vital role in technology and development. There is increased progress in nanotechnology due to the small size (1–100 nm) and unique properties of metallic nanoparticles (NPs), having a higher surface-to-volume ratio, which differentiates them from their bulk properties [1,2]. Metal nanoparticles [3,4] are used in different branches of health and medicine [5,6], photonics [7], sensors [8], and catalyst [9]. The unique optical, electrical, chemical and physical properties depend on the morphology of nanoparticles [10,11], which are further used in various applications, mainly in drug delivery [12,13].

Silver nanoparticles (AgNPs) synthesis was carried out using chemical [14–16] and physical approaches like laser or UV-irradiation [17], microwave irradiation [18], electrochemical reduction [19] and thermal decomposition [20]. It has been found that chemical-based silver nanoparticles are expensive, require high energy consumption [21], and hazardous to animal cells, humans and the environment [22]. To overcome these effects, green synthesis is considered an effective way to reduce the production cost, energy efficiency [23–25], and reduce toxic chemical compounds [26–28]. AgNPs were bio-synthesised with different biomasses like plant extracts [29–32], bacteria, fungi [33,34], algae [35] and other microorganisms [36–38]. To vanquish complicated cell sculpture procedure, synthesis of AgNPs using aqueous leaves extract is preferred [23,27,39]. AgNPs are used in nanotechnology due

to their antioxidant [40–42] antiproliferative [43], antidiabetic [44], antimycotic [45] and anticancer [28,46] properties. AgNPs have good application in water treatment [47], sensors [10,48], treat infections in open wounds [49], mosquito larvicidal [50], and household appliances [51–53].

Various medical plants were used for the synthesis of AgNPs [54–56]. *Kalanchoe pinnata* (*Bryophyllum pinnatum*), commonly known as *patharchat* or *patharkuchi* is a medical plant that belongs to the family of *Crassulaceae* [57] and has been long used in ayurvedic medicine from ancient times. The plant grows in countries like India, Hawaii, Tropical Africa, and Australian continents. Different parts of the plant are used in treatment like stems, leaves, roots, and flowers. The plant leaves contain other properties like antiviral, antimicrobial, anti-inflammatory [58], antitumor, antidiabetic [59], antilithic [60,61], wound healing [62], which is due to the presence of molecular groups in the plant-like alkaloids, phenols and flavonoids, etc.

Dye released from major textile industries and other factories causes severe environmental problems [63,64]. Green technology plays a crucial role in solving this problem by reducing cost and is ecological [65–67]. Synthesized AgNPs are more reactive to the chemical compound because of a higher surface to volume ratio [68] and are used for dye degradation following a photocatalytic reduction under UV-irradiation [69,70]. Rhodamine B (RhB) is a harmful dye to humans, causing harm to the skin and itching in the eyes, and detrimental to aquatic life. Therefore, in the present study, we have used a specific

^{*} Corresponding author.

E-mail address: msmehata@gmail.com (M.S. Mehata).

¹ Both the authors contributed equally.

<https://doi.org/10.1016/j.cplett.2021.138760>

Received 16 April 2021; Received in revised form 16 May 2021; Accepted 18 May 2021

Available online 21 May 2021

0009-2614/© 2021 Elsevier B.V. All rights reserved.

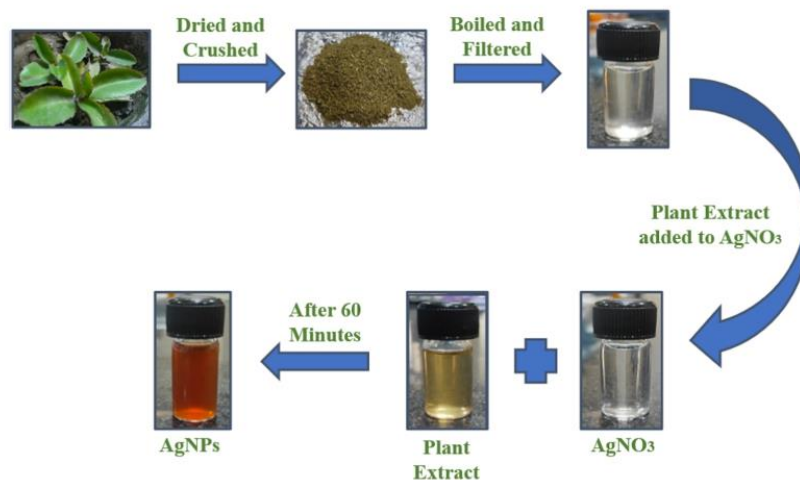


Fig. 1. Schematic representation of synthesized silver nanoparticles using *Kalanchoe pinnata* leaves extract.

plant *Kalanchoe pinnata* leaves extract, to synthesize AgNPs at various physicochemical parameters. The developed AgNPs were used to degrade industrial dye, RhB under UV-irradiation, and antibacterial activities against gram-negative bacterial strain [71].

2. Materials and methods

2.1. Chemicals

Silver nitrate and sodium hydroxide were procured from Aldrich Chem. Co. and the obtained chemicals were utilized without further processing. Ultrapure water (H₂O Adrona B30/integrity+, resistivity 18.2 MΩ cm) was used throughout the study.

2.1.1. Silver nitrate solution

17 mg of AgNO₃ was mixed with 100 mL of ultrapure (UP) water to produce 1 mM of silver nitrate solution. For 2 mM, 3 mM and 4 mM silver nitrate solution 34 mg, 51 mg and 68 mg were added, respectively.

2.2. Preparation of leaves extract

Garden-fresh *Kalanchoe pinnata* (*Bryophyllum pinnatum*) leaves were obtained from the Delhi Technological University campus, which was firstly washed with tap water and further brushed up using the UP water twice; further, leaves were dried and then grinded. 2 g of *Kalanchoe pinnata* powder is dissolved in 50 mL of UP water. The solution was boiled at 60 °C for 15 min before filtered through Whatman filter paper and stored in a cold and dry place for future use.

2.3. AgNPs synthesis using plant leaves extracts

5 mL of plant extract solution was mixed with 45 mL (1 mM) silver salt at 60 °C and stirred for 20 min. On adding plant extract, the colour change was observed. Fig. 1 demonstrates a schematic diagram of

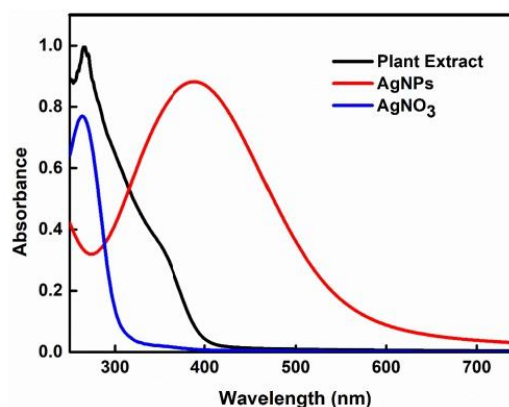


Fig. 2. The absorption spectra of leaves extract, silver salt, and AgNPs synthesized using *Kalanchoe pinnata* leaves extract in an aqueous medium.

synthesized silver nanoparticles.

2.4. Samples for catalysis

4.8 mg of RhB (C₂₀H₃₁ClN₂O₃) dye was added in 10 mL of UP water to make a 10 μM solution. Further, a certain amount of AgNPs (5 mL) was mixed with 25 mL of RhB dye solution (10 μM concentration) and stirred for the next 5 min to achieve an equilibrium state. The dye solution was then transferred into two glass vials, and one of them is stored in a dark room and another is illuminated using UV-light of 8 W and 254 nm (1.2 mW cm⁻²). In both experiments, the amount of AgNPs in the

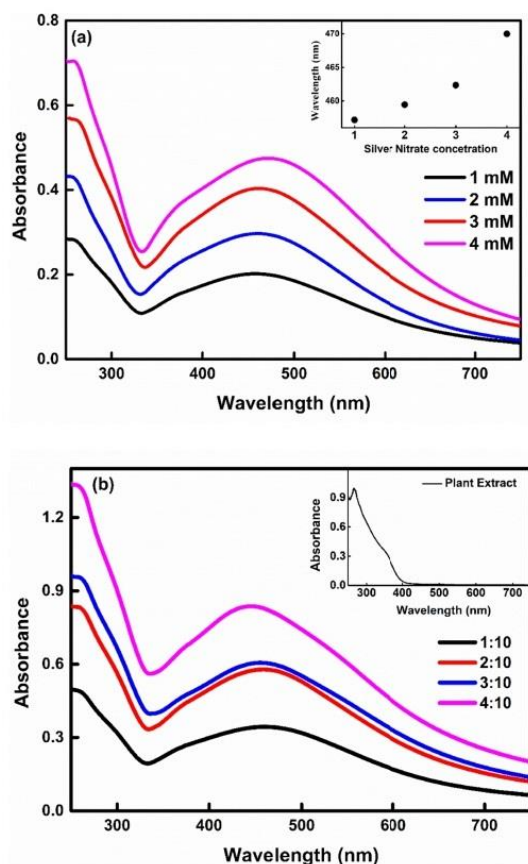


Fig. 3. The absorption spectra of AgNPs at different concentrations of silver salt (a) and with varying ratios of plant extract concentrations (b). Inset of (a) demonstrated the shift in band maximum with the concentration of silver salt at a constant amount of plant extract and (b) the absorption spectrum of plant extract.

dye solution was kept the same.

3. Characterization techniques

For the measurement of absorption spectra, a Perkin Elmer UV/VIS/NIR spectrometer (Lambda 750) was used. The AgNPs dispersed (colloidal AgNPs) in water coated on a glass substrate by a drop-casting method and a thin film was prepared to measure the X-ray diffractogram. X-ray diffractogram of the thin film was recorded by BRUKER-D8 advanced. Zeta potential was recorded using Zetasizer Nano Series ZS particle size and zeta potential Analyzer (Malvern Panalytical). FESEM analysis was done using JEOL JSM-7610F Plus and TEM using TALOS accelerating at a voltage of 200 kV.

4. Results and discussion

The formation and morphology of silver nanoparticles synthesized by *Kalanchoe pinnata* (*Bryophyllum pinnatum*) depend on environmental factors like reaction time, temperature, pH, concentration, etc. Fig. 2 shows the absorption spectra of AgNPs, plant extract and silver salt. A

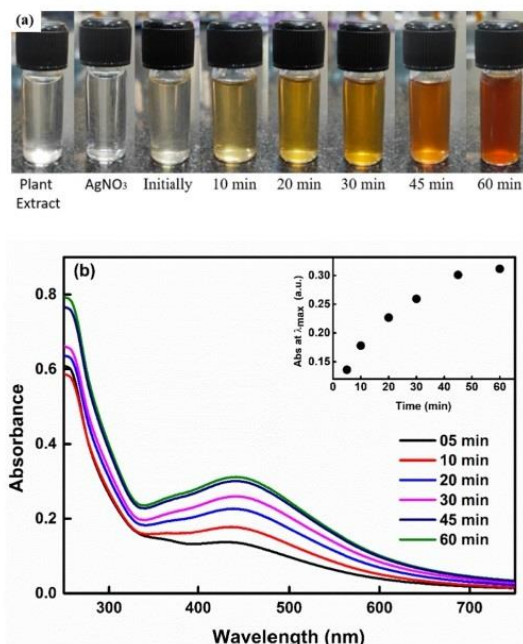


Fig. 4. The colour of the *Kalanchoe pinnata* leaves extract, silver salt, and formation of AgNPs (change in colour) in the water with reaction time (a) and the absorption spectra of AgNPs at different reaction time intervals (b). Inset of (b) shows the increase in absorption intensity with reaction time.

strong band observed at around 430 nm corresponds to the strong surface plasmon resonance (SPR) of the silver nanoparticles. The average particle size of the AgNPs determined using the Mie relation [72] $D = \frac{h\nu_f}{\pi\beta}$ comes out to be 38 nm. Where ν_f ($1.39 \times 10^6 \text{ m sec}^{-1}$) denotes bulk silver electron's fermi velocity, h Planck's constant and β is FWHM (full width at half maximum).

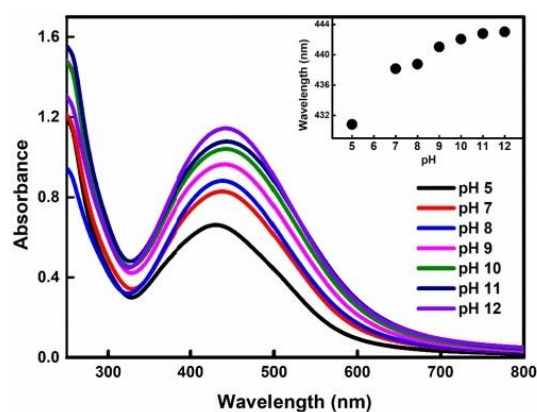


Fig. 5. The absorption spectra of AgNPs in the water at various pH. Inset shows the shift in band maximum as a function of pH.

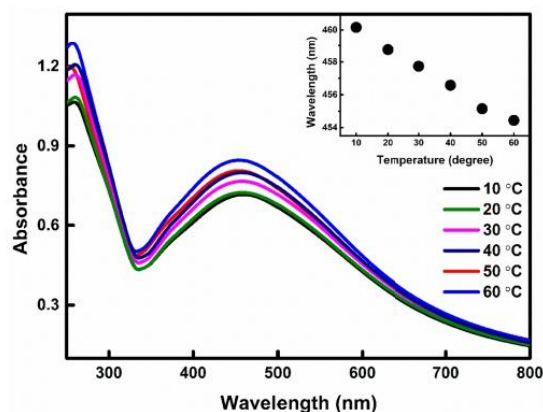


Fig. 6. The absorption spectra of AgNPs in water at various temperatures. Inset shows the shift in band maximum as a function of temperature.

4.1. Effect of silver salt and plant leaves extract concentrations on AgNPs emergence

The emergence of AgNPs was studied at different silver nitrate concentrations (1 mM, 2 mM, 3 mM and 4 mM) and plant extract ratio (1:10, 2:10, 3:10, 4:10) as shown in Fig. 3(a,b). With the increase of the emergence rate of AgNPs, aggregation of nanoparticles was also increased with time, particularly at a higher concentration of precursor salt; hence optimization of concentration is also essential.

4.2. AgNPs formation at different reaction times

When aqueous plant extract was added to 1 mM solution of silver salt, the colour of the solution initially changes light yellow to pale yellow at last into dark brown within an hour, as shown in Fig. 4(a). The colour change of the solution indicates the formation of AgNPs [30]. The plant leaves contain many bio-molecule such as flavonoids, phenols, quinines, etc., which act as reducing and capping agents in the formation and stability of AgNPs. They are accountable for the reduction of Ag^+ to Ag^0 NPs. The maximum colour change of solution occurs within 60 min and no further change in colour observed even after 24 h, indicating the stability of AgNPs. The UV-visible absorption spectra of AgNPs synthesized from *Bryophyllum pinnatum* leaves are shown in Fig. 4b. Thus, the absorption maximum of AgNPs lies between 420 nm and 450 nm and a rise in intensity suggests an enrichment in the AgNPs formation with time.

4.3. Effect of pH on AgNPs formation

pH has a crucial role in changing the shape, size, stability and morphology of AgNPs [73,74]. In some cases, with the increase in pH, the particle size decrease [75]. While in other cases, the size of AgNPs increases with increasing pH, this is due to higher accumulation at lower pH (<5) and lower accumulation at higher pH (6 to 12). This happens due to the existence of particular functional groups in different plants for nucleation [76]. Biomolecules have some electrical charges that were

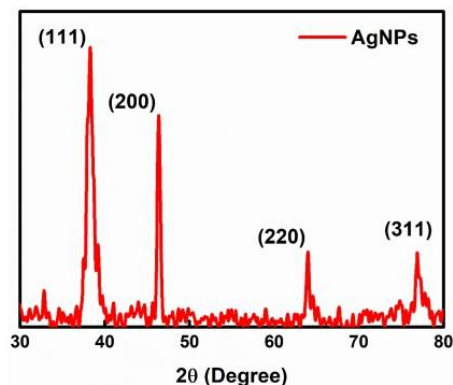


Fig. 7. X-ray diffraction pattern of synthesized AgNPs using *Kalanchoe pinnata* leaves extract.

changed with a change in pH, which might change the properties of capping and stabilizing agents [77]. Fig. 5 shows the absorption spectra of AgNPs at different pH. The absorption intensity increases monotonically with increasing pH. At pH 5, the absorption maximum is at 424 nm, with increasing pH from 5 to 12, the absorption maximum shifted from 420 to 440 nm, resulting in the increase of the size of AgNPs due to a change in the net charge of biomolecules from positive to negative, initiating intense repulsion between the negatively charged ions. The results (Fig. 5) indicate that basic pH is further suitable for AgNPs synthesis [6].

4.4. AgNPs formation at different reaction temperatures

Temperature is a very prominent parameter for determining the morphology of synthesized AgNPs [78]. Fig. 6 shows the absorption spectra of AgNPs at various temperatures from 10 °C to 60 °C in the interval of 10 °C. With the rise in temperature, the reaction rate increases, indicating an increase in the formation of AgNPs due to the increase in the reduction of Ag^+ into Ag^0 [79]. With the increasing temperature, the band maximum shows a blue shift from 440 nm to 420 nm due to the localization of SPR. It implies that the size of NPs decreases with an increase in temperature. With increasing the temperature, the molecules present in the extract solution get higher kinetic energy, resulting in a faster reduction process, indicating no further growth in the size of NPs. Thus, at higher temperatures, small particles with uniform size distribution were formed [12].

4.5. XRD pattern of synthesized AgNPs

Fig. 7 illustrated the XRD pattern of AgNPs (a thin film of AgNPs coated on glass substrate) and indicated the crystalline structure. There are four major reflection peaks at 2θ value of 38.26°, 44.47°, 64.71°, and 76.85°, which are index as (1 1 1), (200), (220), and (3 1 1) planes of the cubic structure of AgNPs (JCPDS, file No. 04-0783) [80,81]. The particle size estimated using Debye-Scherrer's relation $D = 0.9 \lambda / \beta \cos \theta$ corresponding to (1 1 1) peak comes out to 36.9 nm. Here, D represents particle size, λ represents wavelength and β denotes FWHM (full width at

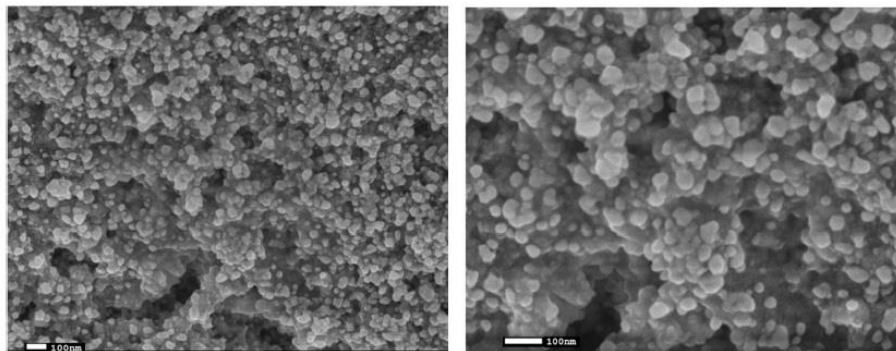


Fig. 8. FESEM images of AgNPs thin film synthesized using *Kalanchoe pinnata* leaves extract.

half maximum) and θ represents Bragg's angle.

4.6. Morphology of silver nanoparticles

The size and shape of synthesized AgNPs were analyzed using FESEM and HRTEM. An aqueous solution of AgNPs was first allowed to settle on a quartz thin film and then FESEM images were taken, as shown in Fig. 8. For HRTEM images (Fig. 9), the AgNPs solution was sonicated and centrifuged, and AgNPs were coated on a copper grid. The broad size distribution of silver nanoparticles was observed and agreed with the observed absorption and Zetasizer [82]. The shape of AgNPs observed from FESEM is spherical, which is in agreement with HRTEM results. Further, EDX analysis (Table 1) confirms the maximum presence of silver. In addition to Ag, Si, and O's existence is due to the use of the substrate, whereas Au is due to the gold coating over the thin film required for FESEM and EDX, as given in Fig. S1 of supplementary materials (SM).

4.7. Zeta potential for silver nanoparticles

Zeta potential affects the suspension stability and particle morphology [83]. It is the measurement of immensity and type of surface charges corresponding to double layer all over the particles with high positive/negative values of zeta potential; accordingly, ± 30 mV is considered a more stable colloidal solution due to electrostatic attraction/repulsion among the particles [84]. It is related to particle size and environmental factors like pH, ionic strength, and the type of ions present in suspension [85]. Fig. 10 illustrates the particle size distribution and the highest intensity appeared for 37.8 nm and 43.8 nm NPs. Thus, the average distribution of AgNPs in colloidal solution is about 40.8 nm and the value of zeta potential is -26.7 mV, indicating higher stability of AgNPs and colloidal dispersion. The details of zeta potential are shown in Fig. S2 of SM.

5. Photocatalytic activity of AgNPs

The photocatalytic behaviour of the AgNPs was examined with the most common laser dye, RhB. The colour of the dye solution is changed from pink to colourless with UV irradiation, as shown in Fig. 11. The colour of the dye solution changed from amber (bright luminescence) to nearly colourless (nearly zero luminescence) under UV irradiation (Fig. S3 of SM). Figs. 12 and 13 show the absorption spectra of RhB dye in dark conditions and under UV irradiation as a function of time. The

absorption spectrum of the dye shows a sharp band at 556 nm corresponds to the n- π transitions (C=N, C=O groups) [69]. In the presence of AgNPs, the absorption intensity decreases. As time passes, the absorption intensity decreases monotonically and becomes minimal within the time of 150 min under dark conditions. The decrease in absorption intensity of the dye under the dark conditions is illustrated in Fig. 12 and UV-irradiation in Fig. 13. Under UV irradiation, the absorption intensity of the dye decreases quite fast by the AgNPs and is reduced entirely in 45 min. Thus, in the dark, the dye degradation process was relatively slow and took more time than dye degradation under UV irradiation. More electrons are available to oxygen from AgNPs under UV irradiation, increasing the reaction process [86]. Apart from decreasing the absorption intensity of the lowest band both in the dark and under UV irradiation, the intermediate absorption band that arises at around 400 nm is significantly affected. Under UV-irradiation, the 414 nm band is pronounced with the passes of time and shifts toward blue (from 434 nm to 414 nm), which is considered to be the SPR band of AgNPs catalysts [87,88], as shown in Fig. S4 of SM. The percentage of dye degradation calculated using $[(C_0 - C_t)/C_0] \times 100$ is about 87% and 83% in the dark (150 min) and under UV-irradiation (45 min), respectively. The term C_t and C_0 represent concentration after time t and initial concentration, respectively.

The reaction rate constant k for dye degradation by AgNPs was estimated with $\ln(C_t/C_0) = -kt$ [88], as shown in Fig. 14, indicating that the dye degradation follows pseudo 1st order kinetics. The k value in the dark is 0.013 min^{-1} and under UV-irradiation is 0.042 min^{-1} . The photocatalytic reduction of dye was observed due to the excitation of SPR in AgNPs [89]. With UV-irradiation, the electron present in the valence band will move towards the conduction band, making a hole (h^+_{VB}) at the lower band and electron (e^-_{CB}) in the upper band [90]. Excited electrons available at AgNPs surfaces interact with oxygen molecules and produce super-oxygen ions ($\cdot O_2^-$) and hydroxyl radicals ($\cdot OH$) [90]. The nanoparticles and radical ions react with dye and degrade it into smaller constituents and in CO_2 and H_2O [68,69,91–94].

6. Antibacterial activity of AgNPs

Bryophyllum pinnatum is known as an herbal plant with leaves having antibacterial properties [95,96]. Plant extract of *Bryophyllum pinnatum* contains photochemical such as flavonoids, polyphenols, terpenoids, alkaloids, and organic acids and are responsible for the biological activity of plant such as antimicrobial and antibacterial. They form complex free radical species with cell membranes affecting the overall

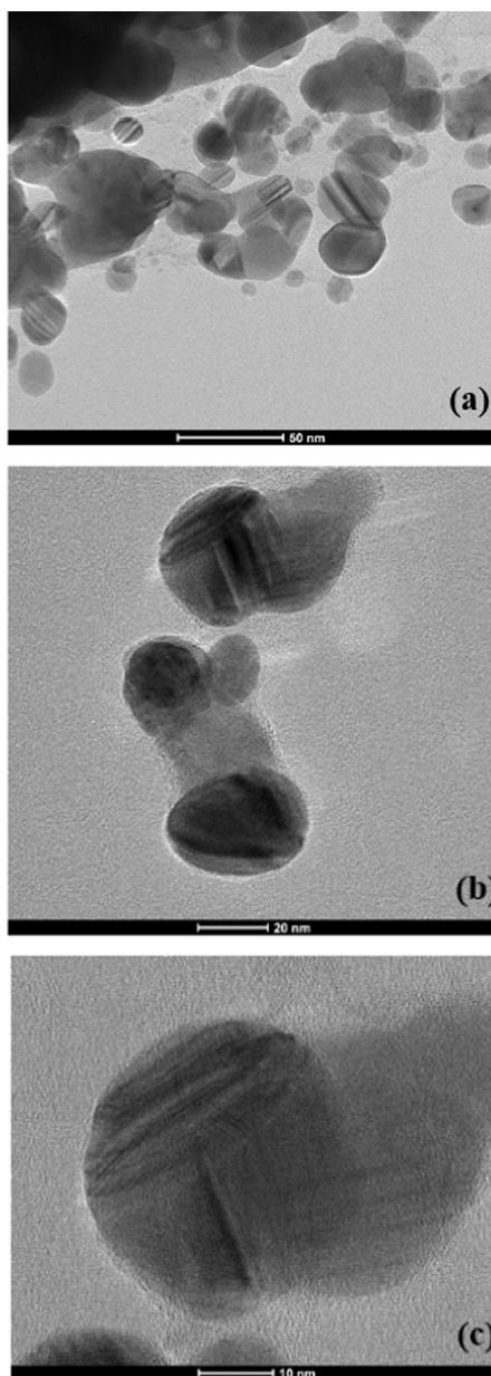


Fig. 9. HRTEM images of AgNPs synthesized using *Kalanchoe pinnata* leaves extract at different magnifications.

Table 1
EDX analysis parameters of AgNPs recorded in thin-film.

Constituent	Weight %	Atomic %
C	4.93	21.65
O	11.10	36.58
Si	0.90	1.69
Au	2.37	0.63
Ag	80.70	39.45

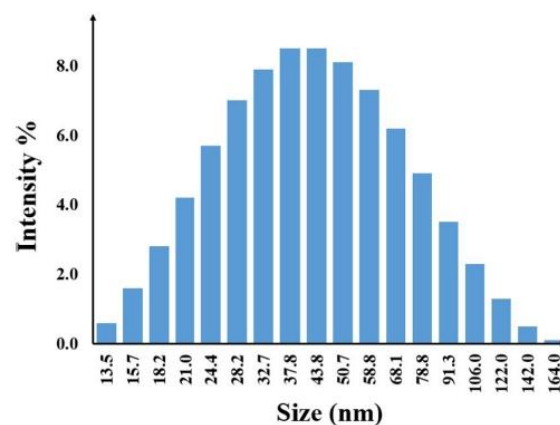


Fig. 10. Particle size distribution for AgNPs synthesized using *Kalanchoe pinnata* leaves extract.

functioning of bacterial cells [5,97]. AgNPs synthesized using *Bryophyllum pinnatum* leaves extract increases antibacterial properties; this is also due to their smaller size and reactivity. The disk diffusion method was used to examine the antibacterial activity of AgNPs against gram-negative bacteria [98]. Fig. 15 shows the antibacterial activities of AgNPs along with the leaves extract and silver salt. The diameter of the zone of inhibition demonstrates the antibacterial property of AgNPs [99], proceeding 36 h in incubation at 37 °C. The zone of inhibition for gram-negative (*E. coli*) is shown in Table 2. It can be seen that a higher zone of inhibition was observed for AgNPs against *E. coli* (gram-negative) bacteria compared to neat plant extract or silver nitrate. Water was taken as standard and silver salt was taken as a control in the antibacterial study. The antibacterial activity of AgNPs was better than AgNO₃ and plant extract because of the smaller size of AgNPs. Smaller AgNPs can penetrate through a more extensive range of bacterial cells, causing a more extensive zone of inhibition of AgNPs. Note that the bacteria are cultured by giving appropriate conditions overnight and were diluted to 1.0×10^{-7} colony. Due to the presence of negative charges on the surface of the cell membrane of bacteria and positive charges like Ag⁺, there is an electrostatic attraction between them, resulting in penetration of the cell membrane. When AgNPs penetrate the cell, they can alter the physical and chemical properties by interacting with the cellular structure and biomolecules of the cell, causing malfunctioning in normal physiological properties such as respiration and permeability of the cell. Further, AgNPs interact with biomolecules of cells forming various oxygen and nitro species that cause stress in the cell's DNA and finally lead to the death of the cell [100,101].

7. Conclusion

AgNPs were synthesized by an eco-friendly and convenient green

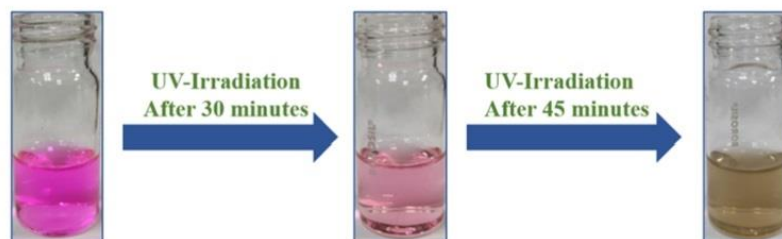


Fig. 11. Change in colour of RhB dye (10 μ M) dissolved in water in the presence of AgNPs with doses of UV-light irradiations.

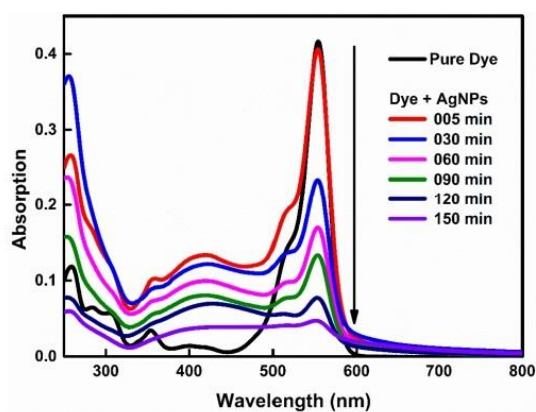


Fig. 12. The absorption spectra of RhB dye in water in the presence of AgNPs at different time intervals in the dark.

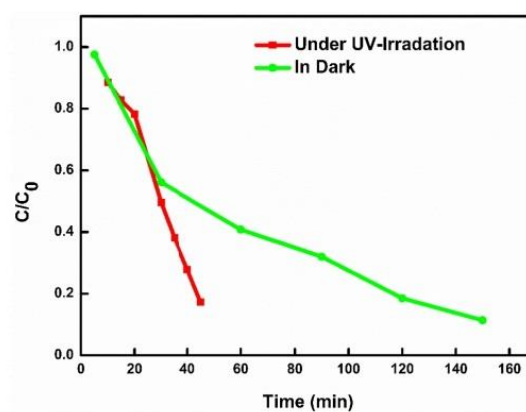


Fig. 14. Plots of C/C_0 against reaction time for reducing RhB dye in the presence of AgNPs in the dark and under UV light.

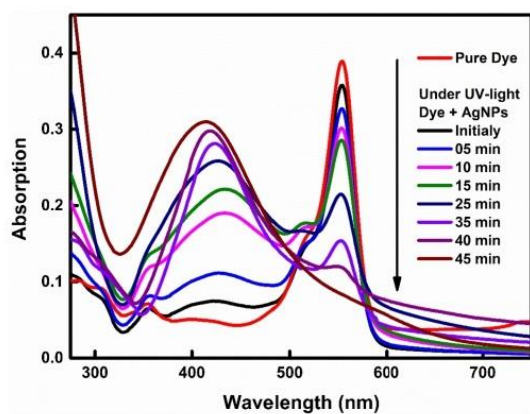


Fig. 13. The absorption spectra of RhB dye in water in the presence of AgNPs at different time intervals under UV irradiation.

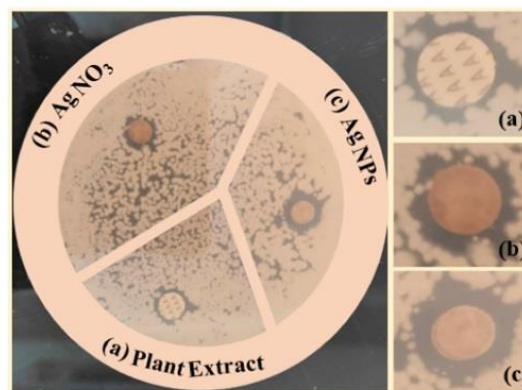


Fig. 15. Zone of inhibition of *E. coli* bacteria treated with *Kalanchoe pinnata* leaves extract (a), silver nitrate (b), and AgNPs (c).

process using the herbal plant *Kalanchoe pinnata* leaves extract. Effect of various parameters like pH, temperature, reactants concentrations and reaction time were studied, confirming the alkaline pH and high temperature were more suitable for the synthesis of AgNPs. A strong SPR band occurs with a maximum between 420 nm and 440 nm. The average size of AgNPs estimated from the absorption spectrum is 38 nm and resembles the XRD, TEM, and SEM results. XRD analysis indicates the crystalline nature of AgNPs, whereas the significant value of zeta

Table 2

Zone of inhibition for plant extract, $AgNO_3$ and AgNPs treated with *E. coli* bacterial strain.

S. No.	Sample Name	Zone of Inhibition (mm)
1	Plant Extract	7.88
2	$AgNO_3$	8.80
3	AgNPs	11.90

potential has proven their high stability. The shape of AgNPs is nearly spherical. The comparison of photocatalyst degradation of RhB dye under UV-light and dark revealed that dye is degraded faster under UV-irradiation. About 83% dye was degraded in 45 min under UV-irradiation with a rate constant (k) of 0.042 min^{-1} and 87% in the dark in 150 min with a k of 0.013 min^{-1} . The value of k is nearly three times higher for dye degradation under UV irradiation than dye degradation in the dark. The bio-synthesized AgNPs reveal enhanced antibacterial activities against *E. coli* bacterial strains. Thus, dye degradation with eco-friendly AgNPs is highly beneficial for industrial applications and its antibacterial activities for medical applications.

CRedit authorship contribution statement

Aryan: Data curation, Formal analysis, Investigation, Methodology, Writing - original draft. **Ruby:** Data curation, Formal analysis, Investigation, Methodology, Writing - original draft. **Mohan Singh Mehata:** Conceptualization, Investigation, Funding acquisition, Resources, Supervision, Validation, Writing - review & editing.

Declaration of Competing Interest

The authors declare that they have no known competing financial interests or personal relationships that could have appeared to influence the work reported in this paper.

Acknowledgment

The authors are grateful to Mr. Mrityunjay Kumar Singh and all the lab members for their help and convenience. The authors extend their gratitude to Ms. Bharti Sharma, Department of Bio and Nano Technology, GJUS&T, for providing the bacterial cultures for antibacterial analysis. The work is financially supported by the Science and Engineering Research Board (EMR/2016/001110), Department of Science and Technology (DST), Govt. of India.

Appendix A. Supplementary data

Supplementary data to this article can be found online at <https://doi.org/10.1016/j.cplett.2021.138760>.

References

- [1] P. Moteriya, S. Chanda, Green synthesis of silver nanoparticles from *Caesalpinia pulcherrima* leaf extract and evaluation of their antimicrobial, cytotoxic and genotoxic potential (3-in-1 system), *J. Inorg. Organomet. Polym. Mater.* 30 (2020) 3920–3932, <https://doi.org/10.1007/s10904-020-01532-7>.
- [2] M. Mazur, Electrochemically prepared silver nanoflakes and nanowires, *Electrochem. Commun.* 6 (2004) 400–403, <https://doi.org/10.1016/j.elecom.2004.02.011>.
- [3] S.S. Shankar, A. Rai, A. Ahmad, M. Sastry, Rapid synthesis of Au, Ag, and bimetallic Au core-Ag shell nanoparticles using Neem (*Azadirachta indica*) leaf broth, *J. Colloid Interface Sci.* 275 (2004) 496–502, <https://doi.org/10.1016/j.jcis.2004.03.003>.
- [4] Y. Yi-Cheun, C. Brian, R.M. Vincet, Gold nanoparticles: preparation, properties, and applications in bionanotechnology, *Nanoscale* 4 (2012) 1871–1880.
- [5] B. Pant, M. Park, G.P. Ojha, D.U. Kim, H.Y. Kim, S.J. Park, Electrospun salicylic acid/polyurethane composite nanofibers for biomedical applications, *Int. J. Polym. Mater. Polym. Biomater.* 67 (2018) 739–744, <https://doi.org/10.1080/00914037.2017.1376200>.
- [6] A. Verma, M.S. Mehata, Controllable synthesis of silver nanoparticles using Neem leaves and their antimicrobial activity, *J. Radiat. Res. Appl. Sci.* 9 (2016) 109–115, <https://doi.org/10.1016/j.jrras.2015.11.001>.
- [7] L. Wei, J. Lu, H. Xu, A. Patel, Z.S. Chen, G. Chen, Silver nanoparticles: synthesis, properties, and therapeutic applications, *Drug Discov. Today* 20 (2015) 595–601, <https://doi.org/10.1016/j.drudis.2014.11.014>.
- [8] S. Unser, I. Bruzas, J. He, L. Sagle, Localized surface plasmon resonance biosensing: current challenges and approaches, *Sensors (Switzerland)* 15 (2015) 15684–15716, <https://doi.org/10.3390/s150715684>.
- [9] G. Merga, R. Wilson, G. Lynn, B.H. Milosavljevic, D. Meisel, Redox catalysis on “naked” silver nanoparticles, *J. Phys. Chem. C* 111 (2007) 12220–12226, <https://doi.org/10.1021/jp074257w>.
- [10] M. Zayats, A.B. Kharitonov, S.P. Pogorelova, O. Lioubashevski, E. Katz, I. Willner, Probing photoelectrochemical processes in Au-QDs nanoparticle arrays by surface plasmon resonance: application for the detection of acetylcholine esterase inhibitors, *J. Am. Chem. Soc.* 125 (2003) 16006–16014, <https://doi.org/10.1021/ja0379215>.
- [11] L. Azeez, A. Lateef, S.A. Adebisi, Silver nanoparticles (AgNPs) biosynthesized using pod extract of *Cola nitida* enhances antioxidant activity and phytochemical composition of *Amaranthus caudatus* Linn, *Appl. Nanosci.* 7 (2017) 59–66, <https://doi.org/10.1007/s13204-017-0546-2>.
- [12] S. Jain, M.S. Mehata, Medicinal plant leaf extract and pure flavonoid mediated green synthesis of silver nanoparticles and their enhanced antibacterial property, *Sci. Rep.* 7 (2017), <https://doi.org/10.1038/s41598-017-15724-3>.
- [13] S.H. Lee, B.H. Jun, Silver nanoparticles: synthesis and application for nanomedicine, *Int. J. Mol. Sci.* 20 (2019) 865–889, <https://doi.org/10.3390/ijms20040865>.
- [14] A.T. Le, L.T. Tam, P.D. Tam, P.T. Huy, T.Q. Huy, N. Van Hieu, A.A. Kudrinskiy, Y. A. Krutyakov, Synthesis of oleic acid-stabilized silver nanoparticles and analysis of their antibacterial activity, *Mater. Sci. Eng. C* 30 (2010) 910–916, <https://doi.org/10.1016/j.msec.2010.04.009>.
- [15] U. Nickel, A.Z. Castell, K. Pöppel, S. Schneider, Silver colloid produced by reduction with hydrazine as support for highly sensitive surface-enhanced Raman spectroscopy, *Langmuir* 16 (2000) 9087–9091, <https://doi.org/10.1021/la000536y>.
- [16] B. Pant, M. Park, S.J. Park, One-step synthesis of silver nanoparticles embedded polyurethane nano-fiber/net structured membrane as an effective antibacterial medium, *Polymers (Basel)* 11 (2019), <https://doi.org/10.3390/polym11071185>.
- [17] N. Marquestaut, Y. Petit, A. Royon, P. Mounaix, T. Cardinal, L. Canonio, Three-dimensional silver nanoparticle formation using femtosecond laser irradiation in phosphate glasses: analogy with photography, *Adv. Funct. Mater.* 24 (2014) 5824–5832, <https://doi.org/10.1002/adfm.201401103>.
- [18] G.A. Kahrilas, W. Haggren, R.L. Read, L.M. Wally, S.J. Fredrick, M. Hiskey, A. L. Prieto, J.E. Owens, Investigation of antibacterial activity by silver nanoparticles prepared by microwave-assisted green syntheses with soluble starch, dextrose, and arabinose, *ACS Sustain. Chem. Eng.* 2 (2014) 590–598, <https://doi.org/10.1021/sc400487x>.
- [19] Y.C. Liu, L.H. Lin, New pathway for the synthesis of ultrafine silver nanoparticles from bulk silver substrates in aqueous solutions by sonochemical methods, *Electrochem. Commun.* 6 (2004) 1163–1168, <https://doi.org/10.1016/j.elecom.2004.09.010>.
- [20] M. Goudarzi, N. Mir, M. Mousavi-Kamazani, S. Bagheri, M. Salavati-Niasari, Biosynthesis and characterization of silver nanoparticles prepared from two novel natural precursors by facile thermal decomposition methods, *Sci. Rep.* 6 (2016) 1–13, <https://doi.org/10.1038/srep32539>.
- [21] P. Mohanpuria, N.K. Rana, S.K. Yadav, Biosynthesis of nanoparticles: technological concepts and future applications, *J. Nanoparticle Res.* 10 (2008) 507–517, <https://doi.org/10.1007/s11051-007-9275-x>.
- [22] R. Bhattacharya, P. Mukherjee, Biological properties of “naked” metal nanoparticles, *Adv. Drug Deliv. Rev.* 60 (2008) 1289–1306, <https://doi.org/10.1016/j.addr.2008.03.013>.
- [23] D. Bose, S. Chatterjee, Biogenic synthesis of silver nanoparticles using guava (*Psidium guajava*) leaf extract and its antibacterial activity against *Pseudomonas aeruginosa*, *Appl. Nanosci.* 6 (2016) 895–901, <https://doi.org/10.1007/s13204-015-0496-5>.
- [24] V. Rangarajan, G. Dhanarajan, P. Dey, D. Chattopadhyay, R. Sen, Bacillus lipopeptides: powerful capping and dispersing agents of silver nanoparticles, *Appl. Nanosci.* 8 (2018) 1809–1821, <https://doi.org/10.1007/s13204-018-0852-3>.
- [25] A. Sengottaiyan, R. Myrthili, T. Selvankumar, A. Aravinthan, S. Kamala-Kannan, K. Manoharan, P. Thyagarajan, M. Govarthanan, J.H. Kim, Green synthesis of silver nanoparticles using *Solanum indicum* L. and their antibacterial, splenocytotoxic potentials, *Res. Chem. Intermed.* 42 (2016) 3095–3103, <https://doi.org/10.1007/s11664-015-2199-7>.
- [26] I.M. Chung, I. Park, K. Seung-Hyun, M. Thiruvengadam, G. Rajakumar, Plant-mediated synthesis of silver nanoparticles: their characteristic properties and therapeutic applications, *Nanoscale Res. Lett.* 11 (2016) 1–14, <https://doi.org/10.1186/s11671-016-1257-4>.
- [27] S. Prabhu, S. Vinodhini, C. Elanchezhian, D. Rajeswari, Evaluation of antidiabetic activity of biologically synthesized silver nanoparticles using *Pouteria sapota* in streptozotocin-induced diabetic rats, *J. Diabetes* 10 (2018) 28–42, <https://doi.org/10.1111/1753-0407.12554>.
- [28] H. Barabadi, M.A. Mahjoub, B. Tajani, A. Ahmadi, Y. Junejo, M. Saravanan, Emerging theranostic biogenic silver nanomaterials for breast cancer: a systematic review, *J. Clust. Sci.* 30 (2019) 259–279, <https://doi.org/10.1007/s10876-018-01491-7>.
- [29] J. Saha, A. Begum, A. Mukherjee, S. Kumar, A novel green synthesis of silver nanoparticles and their catalytic action in reduction of Methylene Blue dye, *Sustain. Environ. Res.* 27 (2017) 245–250, <https://doi.org/10.1016/j.serj.2017.04.003>.
- [30] K. Balan, W. Qing, Y. Wang, X. Liu, T. Palvannan, Y. Wang, F. Ma, Y. Zhang, Antidiabetic activity of silver nanoparticles from green synthesis using *Lonicera japonica* leaf extract, *RSC Adv.* 6 (2016) 40162–40168, <https://doi.org/10.1039/c5ra24391b>.
- [31] H. Bar, D.K. Bhui, G.P. Sahoo, P. Sarkar, S.P. De, A. Misra, Green synthesis of silver nanoparticles using latex of *Jatropha curcas*, *Colloids Surf. A Physicochem. Eng. Asp.* 339 (2009) 134–139, <https://doi.org/10.1016/j.colsurfa.2009.02.008>.